

LOS ALAMOS SCIENTIFIC LABORATORY

OF THE UNIVERSITY OF CALIFORNIA
LOS ALAMOS, NEW MEXICO

CONTRACT W-7405-ENG.36 WITH THE
U.S. ATOMIC ENERGY COMMISSION

LOS ALAMOS NATIONAL LABORATORY



3 9338 00407 9900

THIS DOCUMENT CONTAINS UNCLASSIFIED INFORMATION EXCEPT WHERE SHOWN OTHERWISE. THE DISSEMINATION OF ITS CONTENTS IS UNRESTRICTED.

~~CONFIDENTIAL~~

UNCLASSIFIED

PUBLICLY RELEASABLE
LANL Classification Group

B. J. [unclear]
5/30/96

LOS ALAMOS SCIENTIFIC LABORATORY

of the

UNIVERSITY OF CALIFORNIA

UNCLASSIFIED

Classification changed to
by authority of the U.S. E. R. D. A.,

Report written:
December 9, 1954

Per *L. M. Sabranski, DOC, WHOP, 11/22/76*
(Person authorizing change in classification) (Date)

By *Gate Martinez, 12/8/76*
(Signature of person making the change, and date)

LA-1865

This document consists of 109 pages

EQUATIONS OF STATE FOR HIGH EXPLOSIVES
BASED ON THE KISTIAKOWSKY-WILSON
EQUATION OF STATE FOR THE PRODUCT GASES

C.3

UNCLASSIFIED

~~CONFIDENTIAL~~

UNCLASSIFIED

Work done by:
Robert D. Cowan
Wildon Fickett

Report written by:
Robert D. Cowan
Wildon Fickett

Classification changed by ~~CONFIDENTIAL~~
by authority of the U.S. Atomic Energy Commission

Per *L. M. Redman, 4-8-63*

By REPORT LIBRARY *[Signature]*

TRANSMITTED by authority of
L. M. Redman D-6-1-19-67

By REPORT LIBRARY *[Signature]*
1-24-67

109 pages

~~CONFIDENTIAL~~

UNCLASSIFIED

~~CONFIDENTIAL~~

LOS ALAMOS NATL LAB LIBS
3 9338 00407 9900

SECRET

UNCLASSIFIED

Report distributed: MAR 1 8 1952

AEC Classified Technical Library
University of California Radiation Laboratory, Livermore
Los Alamos Report Library

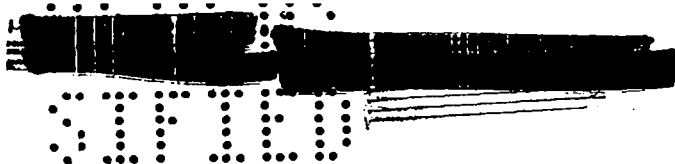
LA-1865

1-7
8
9-30

UNCLASSIFIED

SECRET

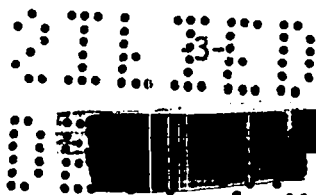
UNCLASSIFIED

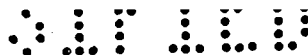
**UNCLASSIFIED**ABSTRACT

A general theory and calculational methods have been developed for the calculation of equation-of-state data for high explosives composed of carbon, hydrogen, nitrogen and oxygen. The theory utilizes the Kistiakowsky-Wilson-Halford equation of state for the gaseous components of the reaction products. The parameters in this equation have been evaluated empirically so as to give results in good agreement with experimental data on the variation of plane-wave detonation velocity with loading density and on Chapman-Jouguet pressure at high loading density for several cyclotols. Detailed equation-of-state data are presented for 65/35 RDX/TNT (Composition B), 77/23 RDX/TNT, 76/24 HMX/TNT, and HMX. The calculated C-J pressure for Composition B is 0.284 Mb, compared with the experimental value 0.292 Mb, and with the value 0.207 Mb for the Jones-Keller equation of state which has been used in the past for implosion calculations.

ACKNOWLEDGEMENTS

The authors are indebted to Frederick R. Parker and Kenneth J. Ewing for help with the machine computations, and to W. W. Wood for several helpful discussions.

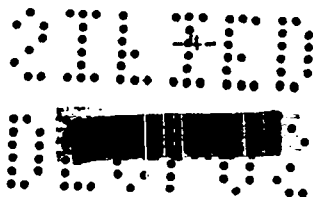
UNCLASSIFIED



UNCLASSIFIED

<u>CONTENTS</u>		Page
Abstract.		3
Acknowledgements		3
Chapter 1. Introduction		7
Chapter 2. Equations of State.		18
2.1 Gaseous Products.		18
2.2 Solid Products (Graphite).		21
Chapter 3. Thermodynamic Theory.		24
3.1 Internal Energy.		25
3.2 Entropy		27
3.3 Chemical Equilibrium		30
Chapter 4. Methods of Calculation		35
4.1 Thermodynamic Data.		35
4.2 Calculation of Equilibrium Composition		38
4.3 Equation-of-State and Detonation-Velocity Calculations.		42
4.4 Internal Consistency		47
Chapter 5. Equation-of-State Parameter Studies.		49
Chapter 6. Determination of Equation-of-State Parameters		60
6.1 Experimental Data		60
6.2 Determination of α and β		64
6.3 Determination of k_1		65
Chapter 7. Results		71
7.1 Equation-of-State Data		71
7.2 Comparison with Experiment		74
7.3 Comparison with Jones-Keller Equation of State		79
7.4 Conclusions		82
References		84
Appendix I. Solution of the Equilibrium Equations.		88
Appendix II. Calculation of Geometrical Covolumes.		91
Appendix III. Equation-of-State Data for Four Explosives		97

UNCLASSIFIED



•••••

UNCLASSIFIED

UNCLASSIFIED

TABLES

	Page
Table 4.1 Analytic Fits for the Equilibrium Constants.	37
Table 4.2 Heats of Formation of Pure Explosives.	37
Table 6.1 Experimental Data for Explosives	61
Table 6.2 Comparison of Covolume Constants	67
Table 7.1 Adiabatic and Shock Hugoniot Through the C-J Point (65/35 RDX/TNT)	75
Table 7.2 Comparison of Calculated C-J Conditions with Experiment.	76
Table II.1 Covolume Constants.	96
Table III.1 Equation of State of 65/35 RDX/TNT	98
Table III.2 Equation of State of 77/23 RDX/TNT	101
Table III.3 Equation of State of 76/24 HMX/TNT	104
Table III.4 Equation of State of HMX	107

UNCLASSIFIED

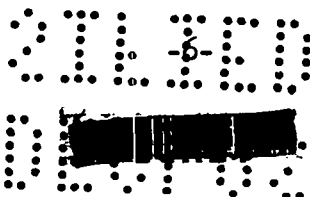
0130
5-
0130



ILLUSTRATIONS

	Page
Fig. 1.1 Hugoniot Curves.	9
Fig. 4.1 Flow diagram of the calculation of thermodynamic variables.	44
Fig. 5.1 Effect of χ on $D - \rho_0$	52
Fig. 5.2 Effect of β on $D - \rho_0$	52
Fig. 5.3 Combined effect of β and χ on $D - \rho_0$	54
Fig. 5.4 Effect of α on $p - \rho_0$ and $T - \rho_0$	54
Fig. 5.5 Effect of α on p ($\rho_0 = 1.715$ g/cc)	56
Fig. 5.6 Effect of α on the C-J shock Hugoniot	56
Fig. 5.7 Effect of graphite equation of state on $D - \rho_0$	58
Fig. 6.1 Comparison of calculated and experimental $D - \rho_0$ curves for "geometrical" k_1	69
Fig. 6.2 Comparison of calculated and experimental $D - \rho_0$ curves for least-square k_1	70
Fig. 7.1 Variation of p_{CJ} and T_{CJ} with ρ_0	72
Fig. 7.2 Variation of C-J composition with ρ_0	73
Fig. 7.3 Variation of composition with volume along detonation Hugoniot and C-J adiabat.	73
Fig. 7.4 Comparison of detonation Hugoniot for 65/35 RDX/TNT with Jones-Keller Hugoniot	80
Fig. 7.5 Comparison of C-J adiabat for 65/35 RDX/TNT with Jones-Keller adiabat	81

UNCLASSIFIED



SECRET

UNCLASSIFIED

Chapter 1

INTRODUCTION

In the past, IBM implosion calculations have utilized an equation of state for the high explosive (Composition B) which was based ultimately on theoretical work by H. Jones and others in England. (19,20) Jones' work provided only the p-v-T relation during adiabatic expansion of the product gases from the Chapman-Jouguet point of the Hugoniot curve. For the implosion runs, the Hugoniot curve itself and adiabats passing through points on the Hugoniot above the C-J point were also required. Peierls and Keller obtained these from Jones' data by perturbation methods, including an approximate conversion of Jones' results for a loading density of 1.5 g/cc to data for the density of 1.67 g/cc in use at that time. The methods employed are described by Keller in LA-1040. (21) By their very nature these methods were not too satisfactory, since the perturbations involved were by no means small. In addition, the production values of loading density and composition have been changed from 1.67 and 60/40 RDX/TNT (by mole fraction) to 1.715 and 65/35 RDX/TNT (by weight), (30) and other explosives than Composition B are contemplated. (a) Accordingly, it seemed desirable to

(a) Kolsky and White (26) have described a method by which they obtained an equation of state for 75/25 RDX/TNT from the Jones-Keller data for Composition B.

UNCLASSIFIED

SECRET

SECRET

UNCLASSIFIED

develop a general theory and calculational methods applicable to any composition and loading density, as well as to make detailed calculations for explosives of current interest. An examination of Jones' theoretical treatment indicated that it would not provide a very satisfactory foundation for this program (for reasons which will be discussed in Section 2.1); an equation of state developed by Kistiakowsky, Wilson, and Halford has therefore been used instead. Before going into any details, however, a summary of the detonation process⁽¹⁴⁾ will be given here for later reference.

Consider a block of (detonating) solid high explosive at a pressure $p_0 = 1$ atm and a specific volume v_0 ($\rho_0 = 1/v_0$ being commonly referred to as the loading density). Advancing through this block with a velocity D is a shock front which compresses the material along the Hugoniot (shock curve) for the solid explosive to a specific volume v_1 (Figure 1.1), thereby raising the pressure to a value p_1 and initiating the chemical reaction. The reaction proceeds through a zone a fraction of a millimeter thick, the completion of the reaction leaving the pressure and volume at a point (p_2, v_2) on the Hugoniot for the reaction products. This is followed by an expansion of the reaction products along the adiabat through (p_2, v_2) . The points (p_0, v_0) , (p_1, v_1) , and (p_2, v_2) are colinear, since it can be shown that the slopes of the lines $(p_0, v_0) \rightarrow (p_1, v_1)$ and $(p_0, v_0) \rightarrow (p_2, v_2)$ are related, respectively, to the velocities of the shock front and the rear of the reaction zone (cf. Eq. 1.2) and these velocities are equal

SECRET

UNCLASSIFIED

SECRET

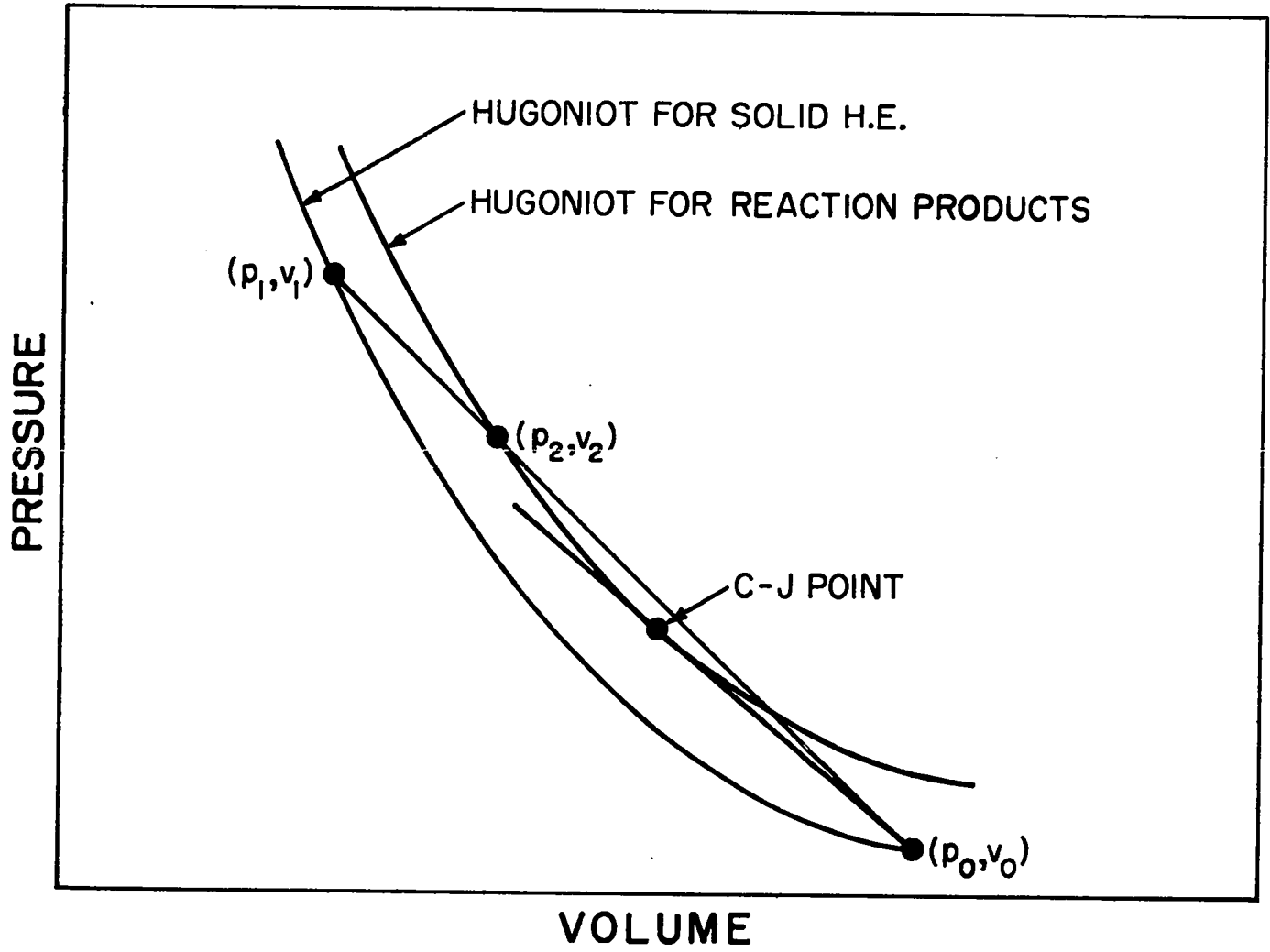
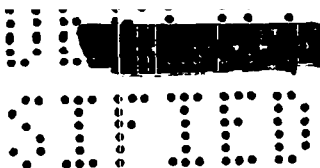


Fig. 1.1 Hugoniot Curves

SECRET



under steady-state conditions.

The laws of conservation of mass and momentum applied across the shock front lead to the following relations

$$\left. \begin{aligned}
 v/v_0 &= \rho_0/\rho = (D - U)/(D - U_0) \\
 p - p_0 &= \rho_0(D - U_0)(U - U_0),
 \end{aligned} \right\} \quad (1.1)$$

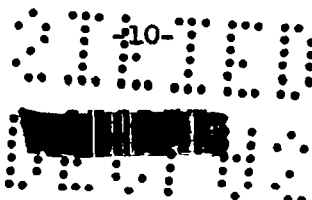
which may be combined to give expressions for the shock (detonation) velocity D and the particle velocity U at the rear of the reaction zone:


$$\left. \begin{aligned}
 D - U_0 &= v_0 \sqrt{(p - p_0)/(v_0 - v)} \\
 U - U_0 &= \sqrt{(p - p_0)(v_0 - v)} .
 \end{aligned} \right\} \quad (1.2)$$

Here (and henceforth) p and v denote the pressure and specific volume of the reaction products -- previously written (p_2, v_2) -- and U_0 is the particle velocity of the material ahead of the shock (and is generally zero).

The law of conservation of energy together with the equations above can be used to derive the so-called Hugoniot equation

$$e - e_0 = \frac{1}{2}(p + p_0)(v_0 - v), \quad (1.3)$$




 5110


where e_0 is the specific internal energy of the solid explosive at (p_0, v_0) and e is the specific internal energy of the reaction products at (p, v) . With the aid of an equation of state for the reaction products (commonly, but misleadingly, referred to as an equation of state of the high explosive), e can be expressed as a function of p and v , which when substituted in (1.3) gives the equation of the Hugoniot curve for the explosion products.


For a plane detonation wave, the well-substantiated hypothesis of Chapman and Jouguet⁽¹⁴⁾ states that the line $(p_0, v_0) \rightarrow (p, v)$ is tangent to the Hugoniot for the explosion products; in this case, the point (p, v) is called the Chapman-Jouguet (C-J) point. In the case of a concave shock front, as in an implosion, the convergence effects may increase the pressure well above the C-J point (as in the case illustrated in Figure 1.1), with a corresponding increase in the detonation velocity D . The plane-wave velocity, for which the Chapman-Jouguet condition is satisfied, will be denoted by D_{CJ} .

The Chapman-Jouguet point possesses several properties of special interest here. First it may be noted that D_{CJ} is the minimum possible value of D . Secondly, the energy change along the Hugoniot is given from Eq. (1.3) by

$$de = \frac{1}{2} \left\{ (v_0 - v) dp - (p + p_0) dv \right\} .$$

Thus from the thermodynamic relation $Tds = de + pdv$ it follows that

5110



 5110

for changes along the Hugoniot,

$$T \left(\frac{ds}{dv} \right)_H = \frac{(v_0 - v)}{2} \left[\left(\frac{dp}{dv} \right)_H - \frac{p - p_0}{v - v_0} \right]. \quad (1.4)$$


Since $(p - p_0)/(v - v_0)$ is the slope of the straight line from (p_0, v_0) to the Hugoniot point (p, v) , it is evident that $(ds/dv)_H \approx 0$ according as $v \approx v_{CJ}$; i.e., the entropy along the Hugoniot curve has a minimum at the Chapman-Jouguet point. This implies that the adiabat (isentropic curve) which passes through the C-J point is tangent to both the Hugoniot curve and the straight line $(p_0, v_0) \rightarrow (p_{CJ}, v_{CJ})$. Thus if γ^* is defined as the negative of the logarithmic slope of an adiabat:

$$\gamma^* = - \left(\frac{\partial \ln p}{\partial \ln v} \right)_s = - \frac{v}{p} \left(\frac{\partial p}{\partial v} \right)_s, \quad (1.5)$$

then at the Chapman-Jouguet point^(a)

$$\gamma^* = - \frac{v}{p} \cdot \frac{p - p_0}{v - v_0} \approx \frac{v}{v_0 - v}, \quad (1.6)$$

^(a) Thus the Chapman-Jouguet condition may be written $(\partial p / \partial v)_s = (p - p_0)/(v - v_0)$. If the composition of the reaction products at each point on the Hugoniot corresponds to chemical equilibrium for that point, then it follows that this derivative should be evaluated along the equilibrium adiabat. However, Kirkwood and Wood⁽²⁴⁾ have recently shown that a correct statement of the C-J condition requires that the derivative be evaluated for frozen composition. All calculated results quoted in this paper are based on the incorrect statement; some check calculations for Composition B have indicated that the resulting error in C-J pressure is completely negligible at high loading density and only about +0.7% at density 1.2 g/cc.

-12-

 5110

~~CONFIDENTIAL~~
 CONFIDENTIAL

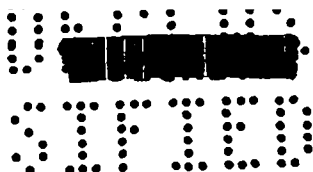
since p_0 is negligible compared with p in the case of a high explosive. From this expression and Eq. (1.2), with $p_0 = U_0 = 0$, there follow the well-known relations

$$\left. \begin{aligned}
 \left(\frac{v}{v_0} \right)_{CJ} &= \frac{\gamma_{CJ}^*}{\gamma_{CJ}^* + 1}, \\
 p_{CJ} &= \frac{p_0 D_{CJ}^2}{\gamma_{CJ}^* + 1}.
 \end{aligned} \right\} \quad (1.7)$$

The Hugoniot and adiabats calculated in the present investigation satisfy all these properties of the C-J point (cf. Sec. 4.4).

As mentioned earlier, a calculation of the Hugoniot curve from Eq. (1.3) requires a knowledge of the equation of state of the detonation products. However, high explosives produce pressures of the order of $1/2 \text{ Mb} \approx 500,000 \text{ atm}$ and volumes of about 10 cc/mole (a 2 or 3 Å cube per molecule), and in this range there exist neither direct experimental data nor a satisfactory self-contained theory. About the best that can be done at the present time is to use some empirical equation of state in which the values of the parameters are chosen so as to give the best possible agreement with the available experimental data on high explosives -- in particular, the velocity of propagation

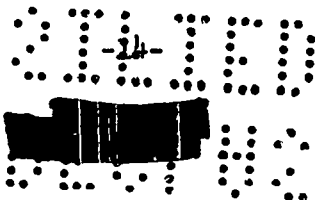
-13-
~~CONFIDENTIAL~~
 CONFIDENTIAL





of a plane detonation wave. As shown by Eq. (1.2), a knowledge of D tells one a little about the Hugoniot -- it is tangent to a certain straight line -- but gives no information at all as to where on the line the tangency occurs nor as to the curvature of the Hugoniot at this point. However, it is possible to press solid explosives to a variety of different densities ρ_0 , and D is found experimentally to increase with ρ_0 . Different values of D mean different slopes of the tangents to the corresponding Hugoniots, and hence give considerably more information than just one value. In fact, if a perfect-gas equation of state is used it can be shown theoretically^(a) that D should be independent of ρ_0 , so that the variation of D with ρ_0 does indeed provide some measure of the gas imperfection terms in the actual equation of state. Accordingly, it has become standard practice to adjust the equation-of-state parameters to give a theoretical curve of D vs. ρ_0 which agrees as closely as possible with the experimental one. This is the procedure which Jones followed, and (in part) the one which is used in this paper (Chapter 6).

Experimental data on the variation of D with ρ_0 are, of course, not sufficient to determine the equation of state uniquely, even in the vicinity of the Chapman-Jouguet points. The information which can be deduced from these data has been discussed by Jones,⁽¹⁸⁾ his arguments

^(a) For example, from Eqs. (1.8) and (1.9) below, using $e = pv/(\gamma^* - 1)$ and neglecting p_0 with respect to p .




 [REDACTED]

 [REDACTED]

being as follows:

The Hugoniot equation (1.3) and the equation for the C-J detonation velocity (1.2) can be written respectively (with $U_0 = 0$ and p_0 assumed constant)

$$\left\{ \begin{array}{l} F(p, v, v_0) = e(p, v) - e_0 - \frac{1}{2}(p + p_0)(v_0 - v) = 0, \\ G(p, v, v_0) = \frac{D_{CJ}^2(v_0)}{v_0^2} (v_0 - v) - (p - p_0) = 0. \end{array} \right.$$


These equations may be thought of as defining two surfaces in a three-dimensional (p, v, v_0) space, the second one being a ruled surface.

These surfaces are tangent to each other along a line which is the locus of Chapman-Jouguet points $p_{CJ}(v_0), v_{CJ}(v_0)$. At any point on this line of tangency the normals to the two surfaces must have the same direction -- thus the projections of the normals on the (v, v_0) plane have the same direction, or

$$\left(\frac{\partial F}{\partial v_0} \right)_{p,v} \div \left(\frac{\partial F}{\partial v} \right)_{p,v_0} = \left(\frac{\partial G}{\partial v_0} \right)_{p,v} \div \left(\frac{\partial G}{\partial v} \right)_{p,v_0} .$$

Evaluation of these derivatives at the C-J pressure, volume, and detonation velocity for the value of v_0 of interest gives

$$\left\{ \frac{1}{2}(p + p_0) \right\}_{CJ} = \left\{ \left[\left(\frac{\partial e}{\partial v} \right)_p + \frac{1}{2}(p + p_0) \right] \left[-1 + 2 \frac{v}{v_0} + 2 \frac{(v_0 - v)}{D} \frac{dD}{dv_0} \right] \right\}_{CJ} .$$

-15-

 [REDACTED]

██████████

Eliminating v with the aid of Eq. (1.7) and letting^(a)

$$\alpha^* = (p + p_0) / \left(\frac{\partial e}{\partial v} \right)_p = (p + p_0) \left(\frac{\partial v}{\partial T} \right)_p / \left(\frac{\partial e}{\partial T} \right)_p, \quad (1.8)$$

this can readily be reduced to

$$\gamma_{CJ}^* + 1 = (2 + \alpha_{CJ}^*) \left(1 + \frac{d \ln D_{CJ}}{d \ln \rho_0} \right). \quad (1.9)$$

Thus, given a value of α_{CJ}^* , this expression together with Eqs. (1.7) gives values of δ^* , v/v_0 , and p at the Chapman-Jouguet point from the experimental variation of D_{CJ} with ρ_0 . Unfortunately, the value of α^* depends on the equation of state. However, it is evident from Eq. (1.8) that $\alpha^* > 0$, and it seems likely that $\alpha^* < 1$. (Jones' estimate is 0.25, the ideal-gas value for diatomic molecules at C-J temperatures is about 1/3, and experimental values for five explosives, Table 7.2, range from 0.28 to 0.70.) Thus if a value $\alpha^* = 1/2$ is assumed, the error in $2 + \alpha^*$ would probably be at most 20%, so that γ_{CJ}^* , p_{CJ} , and $(v/v_0)_{CJ}$ could be predicted from the experimental $D_{CJ} - \rho_0$ data within about 25, 20, and 5%, respectively. In any

^(a)Equivalent expressions (neglecting p_0) are $\alpha^* = \left\{ \left[\gamma_{CJ}^* / \left(\frac{\partial pv}{\partial T} \right)_v \right] - 1 \right\}^{-1}$

$$= \left\{ \left[c_p / \left(\frac{\partial pv}{\partial T} \right)_p \right] - 1 \right\}^{-1}.$$

SECRET

case, the minimum value $\alpha^* = 0$ provides lower limits on γ_{CJ}^* and $(v/v_0)_{CJ}$ and an upper limit on p_{CJ} . Thus the $D_{CJ} - p_0$ experimental data determine not only the straight line to which the Hugoniot must be tangent, but also certain limits as to the location of the point of tangency. However, there is still no information provided as to the curvature of the Hugoniot at this point.

Further discussions of Jones' equation for the equations of state derived in this report and for the Jones-Keller data of LA-1040 are included in Chapter 7.

In addition to experimental $D - p_0$ data, fairly reliable measurements of C-J pressure have recently been made. These of course provide additional information for calibration of the equation of state. This is discussed fully in Chapter 6.

SECRET

██████████

Chapter 2

EQUATIONS OF STATE

2.1 Gaseous Products

The equation of state which Jones^(19,20) used for the gaseous components of the reaction products was a virial expansion in pressure of the form

$$pV_g = RT + bp + cp^2 + dp^3, \quad (2.1)$$

where V_g is the molar volume of the gaseous portion of the reaction products. (The specific volume of the solid product, carbon, was assumed constant and equal to its value at NTP.) The values of the parameters b , c , and d were determined as described in Chapter 1 to give a good fit with experimental $D - \rho_0$ data at loading densities below about 1.5 g/cc, Eq. (2.1) then giving a value of D about 10% higher than experiment at $\rho_0 = 1.7$. Using Jones' C-J values for Composition B at $\rho_0 = 1.5$ g/cc, the terms of the virial expansion in Eq. (2.1) are (in units of Mb-cc/mole)

$$0.297 + 4.49 - 3.30 + 1.34 .$$

Evidently, the series is not converging rapidly even at this pressure (0.177 Mb), and we are here interested in treating pressures five or

SECRET

ten times greater. Although the convergence would probably be better with values of b , c , and d which gave a better fit with the experimental values of D at high densities, it is obvious that a closed-form equation of state would be more satisfactory.

Further objections to Jones' work are: (a) In his treatment of equilibrium he assumes that molecules of all the compounds present in the gaseous products have identical imperfections, i.e., the same equation of state. (b) His treatment of adiabatic expansion is rather complicated, involving the numerical integration of a differential equation.

For the above reasons, Jones' methods were discarded and an equation of state developed by Kistiakowsky, Wilson, and Halford was used instead.⁽²⁵⁾ This equation has been described and a treatment of equilibrium among the product-gas compounds given by Brinkley and Wilson,⁽²⁾ a theoretical treatment of Hugoniot calculations has been given by the same authors,⁽³⁾ and a treatment of adiabatic expansion has been developed by Kirkwood, Brinkley, and Richardson.⁽²³⁾ Similar and somewhat more elegant treatments have been given by Snay and Stegun.⁽³⁵⁾ The theoretical sections of this paper follow those in the above reports, with some refinements and additions.

The Kistiakowsky-Wilson equation of state (slightly modified by us) for the the gaseous reaction products has the form

SECRET

$$\frac{p V_g}{RT} = F(x) = 1 + x e^{\beta x}, \quad (2.2)$$

where

$$x = \frac{\chi k}{V_g (T + \theta)^\alpha} .$$

In these expressions, V_g is the molar volume of the gaseous products (i.e., the total volume of the reaction products less the volume occupied by any solid products, divided by the number of moles of gas, n_g). The quantity θ is a constant which we have introduced (and given the somewhat arbitrary value 400°K) to prevent p from tending to infinity as T tends to zero; this is discussed further in Chapter 5.

Like the Jones equation of state, Eq. (2.2) has three empirical parameters: α , β , and χ . However, it differs from Jones' not only in being of closed form, but also in that the correction to the ideal-gas form is allowed to be a function of the temperature and also to depend on composition through the "constant" k :

$$k = \sum_g x_i k_i, \quad (2.3)$$

where $x_i = n_i/n_g$ is the mole fraction of the gaseous compound i , k_i is a constant characteristic of that compound, and the summation

is carried only over the gaseous components in the reaction products. The k_i are of the nature of covolumes, as will be seen from the treatment of equilibrium (Eq. 3.27) -- the larger the value of one of the k_i , the smaller the value of the corresponding n_i in the equilibrium mixture. (In the treatments by Brinkley and Wilson, etc., the quantity χ in Eq. (2.2) is omitted, but it has been found convenient to introduce it here to provide in effect a simple means of adjusting the magnitude of k without altering the relative values of the k_i .)

The values of α and β used in applications of this equation of state by Brinkley, Snay, etc., are 0.25 and 0.30, respectively. In the present investigation the values have been changed to 0.5 and 0.09 to improve the agreement between calculation and experiment (Chapters 5 and 6). The covolume values k_i used by others have also seemed unsatisfactory to us (for physical reasons), and we have used instead values derived as described in Chapters 5 and 6. We have made a number of other improvements over previous applications, the most important being a reasonable equation of state for the solid component of the reaction products.

2.2 Solid Products (Graphite)

We shall be interested in treating explosives such that the only solid product is carbon (graphite). Brinkley and Wilson^(2,3) assumed for simplicity in their calculations that the specific volume of the

solid carbon present was constant and equal to the value 0.444 cc/g for graphite at NTP. As shown by Figure 5.7, use of a more realistic equation of state produces an appreciable change in the calculated $D - \rho_0$ curve.^(a) We have used an equation of state of the form described in LA-385⁽²²⁾:

$$p = p_1(\eta) + a(\eta) \cdot T + b(\eta) \cdot T^2, \quad (2.4)$$

where $\eta = \rho/\rho_0$ is the compression of the solid graphite relative to its normal crystal density $\rho_0 = 2.25$ g/cc. For our preliminary calculations, including the parameter studies described in Chapter 5, the following expression was used for the zero-temperature pressure:

$$p_1(\eta) = 4.5978 - 10.3594\eta + 6.7575\eta^2 - 1.0598\eta^3 + 0.0628\eta^4. \quad (2.5)$$

This function differs considerably from that given for carbon in LA-208⁽²⁷⁾ for two reasons: (1) We used more recent Bridgman data⁽¹⁾ for the low-compression end of the curve, and (2) Thomas-Fermi-Dirac calculations made by one of us⁽⁹⁾ indicate the high-compression end of the curve to be in error. However, recent experimental measurements⁽⁴⁰⁾ have indicated that Eq. (2.5) gives much too high values for the pressure, and all final results quoted in Chapters 6 and 7 were calculated using the following analytical expressions:

^(a) Christian and Snay⁽⁷⁾ have also made calculations using a variable carbon volume, but their equation of state was purely hypothetical.

$$\left. \begin{aligned}
 p_1(\eta) &= -2.4673 + 6.7692\eta - 6.9555\eta^2 + 3.0405\eta^3 - 0.3869\eta^4, \\
 a(\eta) &= -0.2267 + 0.2712\eta, \\
 b(\eta) &= 0.08316 - 0.07804\eta^{-1} + 0.03068\eta^{-2},
 \end{aligned} \right\} (2.6)$$

these coefficients giving p in megabars when T is in volts (i.e., in units of $11,605.6^\circ\text{K}$). The expression for $b(\eta)$ is an analytic fit to values of b obtained from the (corrected) TFD zero-temperature pressure as described in LA-385. The function $a(\eta)$ is of a form suggested by Reitz,⁽³²⁾ the second coefficient being $3R\phi_0/2$ and the first being chosen to make $a(1) = 3\alpha/\chi$, where α is the linear coefficient of thermal expansion and χ is the isothermal compressibility at NTP. The range of applicability of these expressions is $0 < T < 2$, $0.95 < \eta < 2.5$.

Chapter 3

THERMODYNAMIC THEORY

The calculations described in Chapter 4 require a knowledge of the extensive thermodynamic properties of the detonation products. Since most of the calculations are for a system in chemical equilibrium, the equations determining the composition are also needed.

In general we will be dealing with a gas-solid mixture, for which specific quantities (per unit mass) are most convenient. In deriving the properties for the separate phases, however, it is convenient to use molar quantities. The relation between the two is

$$g = n_g G_g + n_s G_s, \quad (3.1)$$

where g and G represent any extensive property in specific and molar units, respectively; the subscripts g and s refer to gas and solid; and n_g and n_s are the number of moles of gas and solid, respectively, per unit mass of mixture. We wish to derive expressions from which G_g and G_s can be calculated for substances obeying the equations of state (2.2) and (2.4) in terms of tabulated data for the pure components in their standard reference states (ideal gas or real solid at unit pressure).

3.1 Internal Energy

The dependence of internal energy on volume is given by the thermodynamic relation^(a)

$$\left(\frac{\partial E}{\partial V}\right)_T = T \left(\frac{\partial p}{\partial T}\right)_V - p.$$

Integration of this expression at constant temperature and fixed composition then gives the energy of a system at temperature and volume (T, V) in terms of its energy at temperature T and a reference volume V^* :

$$E(T, V) = E(T, V^*) + \int_{V^*}^V \left\{ T \left(\frac{\partial p}{\partial T}\right)_V - p \right\} dv. \quad (3.2)$$

Gaseous components

The standard reference state of ideal gas at unit pressure is equivalent, in the case of internal energy, to ideal (or real) gas at zero pressure. Taking, then, the limit $V^* \rightarrow \infty$, the term $E(T, V^*)$ in Eq. (3.2) may be written as a simple sum of the internal energies of the component substances:

^(a) See, for example, Rossini,⁽³³⁾ Chapter 14.

SECRET

$$E_g(T, \infty) = \sum_i x_i (E_T^0)_i = \sum_i x_i (E_T^0 - H_O^0)_i + \sum_i x_i (H_O^0)_i, \quad (3.3)$$

where $x_i = n_i/n_g$ is the mole fraction of component i and the sum is over all gaseous components of the mixture.

For the equation of state (2.2),

$$\left(\frac{\partial p}{\partial T}\right)_{V_g} = \frac{p}{T} - \frac{\alpha RT x}{V_g(T + \theta)} \frac{dF}{dx} = \frac{p}{T} + \frac{\alpha RT}{T + \theta} \left(\frac{dF}{dV_g}\right)_T, \quad (3.4)$$

since at constant temperature and composition

$$dx = -x dV_g/V_g. \quad (3.5)$$

The integral in (3.2) can thus be written

$$\frac{\alpha RT^2}{T + \theta} \int_{\infty}^{V_g} \left(\frac{dF}{dV_g}\right)_T dV_g = \frac{\alpha RT^2}{T + \theta} \int_1^F dF = \frac{\alpha RT^2}{T + \theta} (F - 1). \quad (3.6)$$

Substitution of (3.3) and (3.6) in (3.2) then gives

$$\frac{E_g(T, V)}{RT} = \sum_i x_i \frac{(E^0 - H_O^0)_i}{RT} + \sum_i x_i \frac{(H_O^0)_i}{RT} + \frac{\alpha T}{T + \theta} (F - 1). \quad (3.7)$$

Solid component

For a solid, the standard reference state is at unit pressure.

SECRET

Taking, therefore, $V^* = V_s^0$ to be the (molar) volume of the solid at temperature T and unit pressure p^0 , (3.2) can be written (for a single solid component)

$$E_s(T, V) = (H_T^0 - H_O^0)_s + (H_O^0)_s - p^0 V_s^0 + \int_{V_s^0}^{V_s} \left\{ T \left(\frac{\partial p}{\partial T} \right)_V - p \right\} dV, \quad (3.8)$$

or, for the solid equation of state (2.4), (a)

$$\frac{E_s(T, V)}{RT} = \frac{(H^0 - H_O^0)_s}{RT} + \frac{(H_O^0)_s}{RT} - \frac{p^0 V_s^0}{RT} + \frac{1}{RT} \int_{V_s^0}^{V_s} \left\{ b(V) T^2 - p_1(V) \right\} dV. \quad (3.9)$$

3.2 Entropy

The pressure dependence of entropy is given by the thermodynamic relation (b)

$$\left(\frac{\partial S}{\partial p} \right)_T = - \left(\frac{\partial V}{\partial T} \right)_p.$$

(a) In evaluating the thermodynamic functions for the solid (Eqs. 3.9, 3.18, and 3.24) we have neglected $p^0 V_s^0$ and approximated $V_s^0 = V_s^0(T)$ by the constant value $V_s^0(25^\circ\text{C})$; the resulting errors are less than those of the analytic fit which we used for $H^0 - H_O^0$.

(b) See, for example, Rossini, (33) Chapter 13.

[REDACTED]

Integrating at constant temperature and fixed composition from the reference pressure $p^{\circ} = 1 \text{ atm}$ gives

$$S(T, p) = S(T, p^{\circ}) - \int_{p^{\circ}}^p \left(\frac{\partial V}{\partial T} \right)_p dp. \quad (3.10)$$

Gaseous components

The entropy of a real gas at (T, p) may be expressed in terms of the entropy of the ideal gas at (T, p°) through the relation^(a)

$$S_g(T, p) = S_I(T, p^{\circ}) + \int_0^{p^{\circ}} \left\{ \frac{R}{p} - \left(\frac{\partial V}{\partial T} \right)_p \right\} dp, \quad (3.11)$$

and the entropy S_I of the mixture of ideal gases is in turn related to the entropies of the pure components, each at pressure p° , by

$$S_I(T, p^{\circ}) = \sum_i x_i (S^{\circ})_i - R \sum_i x_i \ln x_i, \quad (3.12)$$

where the second sum represents the entropy of mixing. Combining (3.11) and (3.12) with (3.10) gives for the gaseous mixture,

$$\frac{S_g(T, p)}{R} = \sum_i x_i \frac{(S^{\circ})_i}{R} - \sum_i x_i \ln x_i - \ln \frac{p}{p^{\circ}} + \int_0^{p^{\circ}} \left\{ \frac{1}{p} - \frac{1}{R} \left(\frac{\partial V_g}{\partial T} \right)_p \right\} dp. \quad (3.13)$$

For the equation of state (2.2), it is convenient to transform

^(a) Rossini, (33) Chapter 23, Eq. (42).

[REDACTED]

the integral in (3.13) with the aid of the differential relation

$$\left(\frac{\partial v}{\partial T}\right)_p = -\left(\frac{\partial v}{\partial p}\right)_T \left(\frac{\partial p}{\partial T}\right)_v. \quad (3.14)$$

Using (3.4)(3.5), and the following relation for constant temperature and composition:

$$\frac{dp}{p} = \frac{dF}{F} - \frac{dv_g}{v_g}, \quad (3.15)$$

the integral in (3.13) can be written

$$\begin{aligned} \int_1^F \frac{dF}{F} + \int_{\infty}^{v_g} \left\{ \frac{F-1}{v_g} + \frac{\alpha T}{T+\theta} \left(\frac{dF}{dv_g}\right)_T \right\} dv_g \\ = \ln F - \int_0^x e^{\beta x} dx + \frac{\alpha T}{T+\theta} \int_1^F dF. \end{aligned}$$

Thus we obtain for the entropy of the gaseous components of the mixture:

$$\begin{aligned} \frac{S_g}{R} = \sum_i x_i \frac{(S^0)_i}{R} - \sum_i x_i \ln x_i - \ln \frac{p}{p^0} \\ + \ln F - \frac{e^{\beta x} - 1}{\beta} + \frac{\alpha T}{T+\theta} (F-1). \end{aligned} \quad (3.16)$$



Solid component

Converting the integral in (3.10) with the aid of the relation (3.14), the entropy of the solid component can be written

$$S(T, v_s) = (S^0)_s + \int_{V_s^0}^{V_s} \left(\frac{\partial p}{\partial T} \right)_{V_s} dV_s, \quad (3.17)$$

where V_s^0 is as before the (molar) volume of the solid at temperature T and unit pressure p^0 . For the solid equation of state (2.4), this becomes

$$\frac{S_s}{R} = \frac{(S^0)_s}{R} + \frac{1}{R} \int_{V_s^0}^{V_s} \{ a(V) + 2b(V) T \} dV. \quad (3.18)$$

3.3 Chemical Equilibrium

The equilibrium state of a system is characterized by the possibility of a number of chemical reactions among the components, each reaction being subject to the thermodynamic condition

$$\sum_i \nu_i \mu_i = 0. \quad (3.19)$$

Here ν_i is the number of moles of component i involved in the reaction, ν_i being positive for products and negative for reactants, and



$$\mu_i = \left(\frac{\partial(nA)}{\partial n_i} \right)_{T,v,n_j} = \left(\frac{\partial(nF)}{\partial n_i} \right)_{T,p,n_j} \quad (3.20)$$

is the chemical potential of component i . (The subscripts v and n_j indicate differentiation with total volume and all n 's other than n_i held constant.) ^(a)

The conditions for the conservation of mass, together with all independent equations of the type (3.19) are just sufficient to determine the composition of the system, provided that the chemical potentials of the components are known.

Gaseous components

For the gaseous components obeying the equation of state (2.2), μ_i is most easily found from the work function A , which from (3.7) and (3.16) may be written (since $E^0/RT - S^0/R = F^0/RT - 1$),

$$\begin{aligned} \frac{n A}{g g} &= \frac{n E}{g g} - \frac{n S}{R} \\ &= \sum_i n_i \frac{(F^0 - H^0)_i}{RT} + \sum_i n_i \frac{(H^0)_i}{RT} - n_g + \sum_i n_i \ln n_i \\ &\quad + n_g \ln \frac{p}{n_g p^0} + n_g \frac{e^{\beta x} - 1}{\beta} \end{aligned}$$

^(a) Here A and F are the molar Helmholtz and Gibbs free energies, respectively. This F should not be confused with that in Eq. (2.2).



From (3.20) we then have for the chemical potential of the i^{th} gaseous component

$$\begin{aligned} \frac{\mu_i}{RT} &= \frac{(F^{\circ} - H^{\circ}_O)_i}{RT} + \frac{(H^{\circ}_O)_i}{RT} + \ln n_i + \ln \frac{p}{n_g p^{\circ}_F} + \frac{e^{\beta x} - 1}{\beta} + n_g e^{\beta x} \left(\frac{\partial x}{\partial n_i} \right)_{T, V_g, n_j} \\ &= \frac{(F^{\circ} - H^{\circ}_O)_i}{RT} + \frac{(H^{\circ}_O)_i}{RT} + \ln \frac{x_i p}{p^{\circ}} + \frac{e^{\beta x} - 1}{\beta} - \ln F + \frac{k_i}{k} (F - 1). \quad (3.21) \end{aligned}$$

Solid component

For the solid component, the chemical potential is more easily found from the free energy F , which from (3.8) and (3.17) may be written

$$\begin{aligned} \frac{n_s F_s}{RT} &= \frac{n_s E_s + n_s p V_s}{RT} - \frac{n_s S_s}{R} \\ &= \frac{n_s (F^{\circ} - H^{\circ}_O)_s}{RT} + \frac{n_s (H^{\circ}_O)_s}{RT} + \frac{n_s (p V_s - p^{\circ} V^{\circ}_s)}{RT} - \frac{n_s}{RT} \int_{V^{\circ}_s}^{V_s} p \, dV. \quad (3.22) \end{aligned}$$

Thus from (3.20), the chemical potential of the solid component is

$$\frac{\mu_s}{RT} = \frac{(F^{\circ} - H^{\circ}_O)_s}{RT} + \frac{(H^{\circ}_O)_s}{RT} + \frac{F'_s}{RT}, \quad (3.23)$$

where for the equation of state (2.4),



$$\begin{aligned} \frac{F'_s}{RT} &= \frac{p V_s - p^o V_s^o}{RT} - \frac{1}{RT} \int_{V_s^o}^{V_s} p \, dV \\ &= \frac{p V_s - p^o V_s^o}{RT} - \frac{1}{RT} \int_{V_s^o}^{V_s} \left\{ p_1(V) + a(V) T + b(V) T^2 \right\} dV. \end{aligned} \quad (3.24)$$

Equilibrium conditions

The equilibrium condition (3.19) for the $\underline{m}^{\text{th}}$ chemical reaction may now be written with the aid of (3.21) and (3.23) as

$$\begin{aligned} \sum_i (\nu_i)_m \mu_i &= \sum_i (\nu_i)_m \frac{(F^o - H^o)_i}{RT} + \sum_i (\nu_i)_m \frac{(H^o)_i}{RT} + \sum_g (\nu_i)_m \ln n_i \\ &+ \left(\sum_g \nu_i \right)_m \left\{ \ln \frac{p}{p^o n_g^F} + \frac{e^{\beta x} - 1}{\beta} \right\} + \left(\sum_g \nu_i k_i \right)_m \frac{(F - 1)}{k} \\ &+ \frac{(\nu_s)_m F'_s}{RT} = 0. \end{aligned} \quad (3.25)$$

Making use of the definition of the equilibrium constant K_p :

$$\ln(K_p)_m = - \sum_i (\nu_i)_m \frac{(F^o - H^o)_i}{RT} - \sum_i (\nu_i)_m \frac{(H^o)_i}{RT}, \quad (3.26)$$

we obtain the following equilibrium condition for the $\underline{m}^{\text{th}}$ reaction:

$$\begin{aligned}
 \ln K_m &= \ln(\pi_g n_i^{(v)_i}_m) \\
 &= \ln (K_p)_m - (\sum_g v_i)_m \left\{ \ln \frac{p}{p^0 n_g^F} + \frac{e^{\beta x} - 1}{\beta} \right\} \\
 &\quad - (\sum_g v_i k_i)_m \frac{(F - 1)}{k} - \frac{(v_s)_m F'_s}{RT} .
 \end{aligned} \tag{3.27}$$

[REDACTED]

Chapter 4

METHODS OF CALCULATION

4.1 Thermodynamic Data

The numerical calculations described below are rather complex, and were carried out on IBM Type 701 Electronic Data Processing Machines. These calculations require (Eqs. 3.7, 3.9, 3.16, 3.18, 3.26) values of the thermodynamic quantities E° , S° , and $\ln K_p$ for various substances and reactions over an extended temperature range -- preferably in the form of analytic fits. It is desirable that fits for E° and S° be consistent with the thermodynamic relation

$$T dS^\circ = dE^\circ + p^\circ dV = \begin{cases} dE^\circ + R dT, & \text{gas} \\ dH^\circ & , \text{solid} \end{cases}$$

so as to insure correct relationships between calculated shock curves and adiabats. Such fits have been given by us⁽¹³⁾ in the forms

$$\text{Gas: } \begin{cases} (E^\circ - H^\circ_0)/RT = a + bT + cT^2 + dT^3 \\ S^\circ/R = (a + 1) \ln T + 2bT + \frac{3}{2}cT^2 + \frac{4}{3}dT^3 + e, \end{cases} \quad (4.1)$$

██████████

$$\text{Solid: } \left\{ \begin{array}{l} (H^{\circ} - H_{\circ}^{\circ})/RT = a + bT + cT^2 + dT^3 \\ S^{\circ}/R = a \ln T + 2bT + \frac{3}{2} cT^2 + \frac{4}{3} dT^3 + e. \end{array} \right. \quad (4.2)$$

Analytic fits for $\ln K_p$ could have been made by combining these expressions according to the definition (3.26) and the relation

$$(F^{\circ} - H_{\circ}^{\circ})/RT = \left\{ \begin{array}{l} (E^{\circ} - H_{\circ}^{\circ})/RT - S^{\circ}/R + 1, \text{ gas} \\ (H^{\circ} - H_{\circ}^{\circ})/RT - S^{\circ}/R, \text{ solid.} \end{array} \right.$$

However, for simplicity the free energy was fit with simple cubic expressions of the form used for the energy. This is not thermodynamically consistent, but is satisfactory for our purposes. Values of the coefficients for the $\ln K_p$ fits are given in Table 4.1.

Values are also required for the heats of formation of the various explosives (cf. Eq. 4.9), and these are given in Table 4.2. Heats of formation, H_{\circ}° , for the reaction products at $T = 0^{\circ}\text{K}$ and heat contents, $H_{T_0}^{\circ} - H_{\circ}^{\circ}$, for the elements making up the explosive were taken from the NBS tables.⁽³⁸⁾ (All internal energies quoted in this paper are thus referred to an energy zero such that the energies of the elements are zero at $T = 0^{\circ}\text{K}$.) The values $R = 1.98719 \text{ cal/mole} = 8.31439 \times 10^{-5} \text{ Mb-cc/mole}$ were also taken from the NBS tables.

██████████



Table 4.1

Analytic Fits for the Equilibrium Constants: (a)

$$\ln(K_p)_m = a_m + b_m T + c_m T^2 + d_m T^3 - (\Delta H^{\circ}_O)_m / RT$$

Range, 500 to 3000°K

<u>m</u>	<u>a_m</u>	<u>b_m · 10⁴</u>	<u>c_m · 10⁸</u>	<u>d_m · 10¹²</u>	<u>(ΔH^o_O)_m / R</u>
1	5.2269	-7.6124	6.7274	1.8218	4,861.0
2	5.0679	26.8080	-87.1936	102.1230	39,545.3
3	-18.5737	-31.1507	139.0486	-182.5956	-19,909.9

Range, 3000 to 12000°K

1	4.7051	-4.6135	3.3830	-1.0266	4,861.0
2	7.2128	3.8783	-4.4698	1.7107	39,545.3
3	-21.2756	3.1990	-0.0672	-0.4704	-19,909.9

Table 4.2

Heats of Formation of Pure Explosives

(ΔH_f)_e

<u>Explosive</u>	<u>(kcal /mole at 25°c)</u>
HMX (C ₄ H ₈ N ₈ O ₈)	+17.93 (17)
RDX (C ₃ H ₆ N ₆ O ₆)	+14.71 (31)
TNT (C ₇ H ₅ N ₃ O ₆)	-17.81 (36)
DNPA (C ₆ H ₈ N ₂ O ₆)	-121.2 (b, 34)

(a) The reactions m are defined by (4.5).

(b) Poly-dinitropropylacrylate (per polymer unit).





4.2 Calculation of Equilibrium Composition

We consider only explosives containing C, H, N, and O, and giving the following reaction products:

<u>i</u>	<u>Substance</u>	
(1)	H ₂	} (4.3)
(2)	CO ₂	
(3)	CO	
(4)	H ₂ O	
(5)	N ₂	
(6)	NO	
(7)	C(s)	

In reducing the number of chemical components considered to a computationally practical minimum, the following considerations served as a guide:

(a) In addition to the simple, stable components commonly thought to be present (CO, H₂O, N₂, C(s)), there should be another nitrogen and another hydrogen compound in order that neither the amount of N₂ nor H₂O should be automatically fixed.

(b) The list should include components which will be representative of the effects of molecular size and heat of formation.





(c) The list should be as short as possible, and the component subscripts for each molecule should have as small a ratio as possible consistent with (a). (For example, NH_3 or CH_4 is likely to introduce more complication into the equations than H_2O .)

Thus the list contains, in addition to CO , H_2O , N_2 , and C(s) three others: H_2 (small size), CO_2 (large size), and NO (positive heat of formation).

Since the calculated composition depends rather strongly on the values of the covolumes, whose choice is somewhat arbitrary, the computational cost of including more components is probably not justified. In some preliminary calculations (on IBM-CPC equipment) OH , NH_3 , and CH_4 were also included.^(a) Although these compounds were usually found to be present in appreciable amounts (e.g., mole fractions of 1 to 10%), they were omitted in the final calculations for the reasons given above. It should be noted that our set of components would probably not be suitable for an explosive more oxygen-rich than RDX (which balances to CO , H_2O , and N_2) since the absence of O_2 would force the burning of N_2 or CO .

The conservation equations for the four elements present are

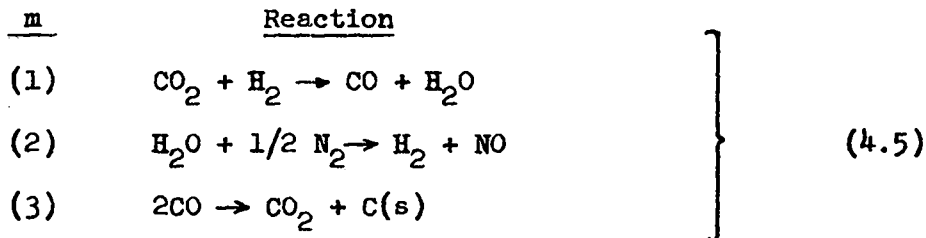
^(a) These molecules were included in the list of reaction products considered by Kirkwood, et al.⁽²³⁾



$$\begin{aligned}
 n_2 + n_3 + n_7 &= N_C, \\
 2n_1 + 2n_4 &= N_H, \\
 2n_5 + n_6 &= N_N, \\
 2n_2 + n_3 + n_4 + n_6 &= N_O,
 \end{aligned}
 \tag{4.4}$$

where the n_i are the numbers of moles of the components in the product mixture per unit mass of explosive— n_1 being the number of moles of hydrogen, and similarly for the remaining numerical subscripts, following the list (4.3) of components. The N_C , N_H , N_N , N_O are the numbers of gram-atoms of C, H, N, and O, respectively, per unit mass of explosive.

The reactions considered were as follows:



(Any other set of three independent reactions involving these components could of course have been used; however, it is desirable that only one of them involve solid carbon.)

Corresponding to these reactions we have the following



equilibrium equations:

$$\left. \begin{aligned}
 K_1 &= \frac{n_3 n_4}{n_1 n_2} \\
 K_2 &= \frac{n_1 n_6}{n_4 (n_5)^{1/2}} \\
 K_3 &= \frac{n_2}{n_3}
 \end{aligned} \right\} \quad (4.6)$$

where the K 's are given by Eq. (3.27), the $(K_p)_m$'s being calculated as indicated in Table 4.1. With solid carbon present, Eqs. (4.4) and (4.6) constitute a system of seven equations in seven unknowns, three equations being non-linear. The method of solution which we used consists essentially of an iteration on the single variable n_3 , and is described in detail in Appendix I.

When the equilibrium Eqs. (4.4) and (4.6) are used to calculate the mole numbers, it is found in some cases that n_7 is negative. This is of course impossible, and means physically that there is no solid carbon present ($n_7 = 0$). Mathematically, the equilibrium equations must be altered by deleting n_7 from the carbon conservation equation and ignoring the equilibrium equation involving K_3 . There remains a system of six equations in the six unknowns n_1, n_2, \dots, n_6 . Solutions were obtained by combining the six equations to the point where they



could be solved by iterating on the single variable n_1 . Details are given in Appendix I.

4.3 Equation-of-State and Detonation-Velocity Calculations

For use in hydrodynamic calculations, the equation of state of the reaction products is needed in the form $p = p(v,e)$ or $p = p(v,s)$ where v is the specific volume of the gas-solid mixture, and e and s are the specific energy and entropy. The determination of functional relations of this sort may be considered as special cases of the calculation of all thermodynamic quantities of interest as a function of v and g , where g may represent any one of the quantities e , s , T , p , or the Hugoniot function h (Eq. 4.8).

To facilitate tabulation of data, curve plotting, and the construction of analytic fits to the data, it is desirable that results be obtained for specified (and round) values of v and g . On the other hand, the equations to be solved are such that it is essential that v and T be taken as independent variables; it is therefore necessary to iterate on the value of T until the specified value of g is obtained. The manner in which this is accomplished is shown schematically in Figure 4.1.

Thus suppose that it is desired to determine the various thermodynamic quantities at some v and g , say g_c . The first step is to guess a temperature and composition (in general, the final values obtained at the previously calculated point). Then the (molar) solid



and gas volumes are determined so that

$$p_g(v_g) = p_s(v_s), \quad (4.7)$$

where $n_g v_g = v - n_s v_s$, and p_g and p_s are the pressures computed from the gas and solid equations of state, (2.2) and (2.4). More precisely, the solid volume v_s is iterated with "linear feedback"⁽²⁸⁾ until (4.7) is satisfied.



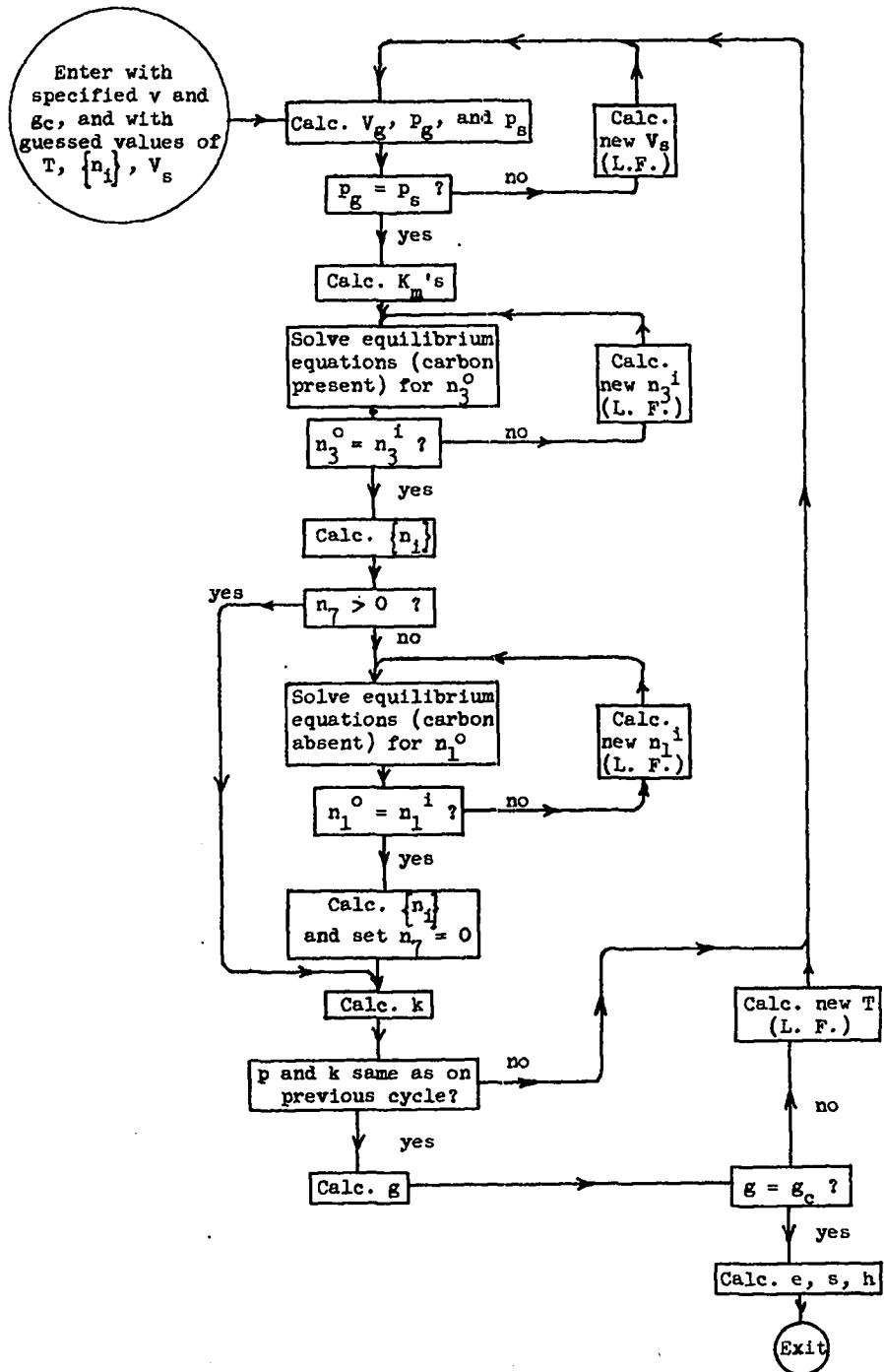


Fig. 4.1. Flow diagram of the calculation of the thermodynamic variables at specified v and g_c . L. F. indicates the application of "linear feedback" to the iteration (see text). The superscripts i and o indicate input and output values, respectively, of n_3 or n_1 .



Having so determined V_s and V_g , we can calculate the K_m 's from (3.27). With these K_m 's the composition is determined by iteration as outlined in Sec. 4.2. With this new composition the gas and solid volumes are redetermined, the K_m 's recomputed, and the composition is again determined so as to satisfy the new K_m 's. When this whole process has converged (i.e., the pressure and composition are no longer changing) g is calculated. In general $g \neq g_c$; T is then changed by linear feedback on g and T and the whole process is repeated until $g = g_c$. With the final T (and p) thus arrived at, e , s , and h are calculated from Eq. (4.8) and the expressions derived in Chapter 3. For the data reported below, all iterations in this process were carried to an accuracy of about one part in 10^5 , and the machine time required for such a calculation at one point (v , g_c) was about twenty seconds.

For the calculation of a Hugoniot curve, g was taken to be the Hugoniot function

$$h = e - e_0 - \frac{1}{2}(p + p_0)(v_0 - v) \quad (4.8)$$

and g_c was taken to be zero (cf. Eq. (1.3)). Here e_0 and v_0 are the specific energy and volume of the material at the starting conditions. For a detonation, e_0 and v_0 refer to the undetonated material; thus v_0 is the reciprocal of the loading density ρ_0 , and



██████████

$$e_o = (\Delta H_f)_e / M_e + \sum N_j (H_{T_o}^o - H_o^o)_j + \sum N_j (H_o^o)_j - p_o v_o, \quad (4.9)$$

where $(\Delta H_f)_e$ is the molar enthalpy of formation of the explosive at T_o (usually 25°C), M_e is the molecular weight of the explosive, and N_j is the number of moles of element j contained in unit mass of explosive. Since the energy of the undetonated explosive and the energy of the reaction products must be referred to the same energy zero, the H_o^o 's in Eqs. (3.7), (3.9), and (4.9) must of course be consistent. The $p_o v_o$ term is small compared to the experimental error in the values of $(\Delta H_f)_e$ available and was neglected.

In order to calculate a C-J detonation velocity, g was taken to be the Hugoniot function, Eq. (4.8), with e_o given by (4.9). Then points were calculated on the detonation Hugoniot until a minimum value of $D = v_o \sqrt{(p - p_o)/(v_o - v)}$ was found. This was done by calculating D at three values of v which bracketed the minimum; then approximating D vs. v with a parabola through these three points and taking the analytically predicted volume for minimum D as the middle volume for the next guess. This was repeated with successively finer volume intervals until the volume for minimum D had been determined to the desired accuracy. For maximum loading density, the volume was determined to 1 part in 10^5 and required about 5 minutes machine time; for lower densities the accuracy was about 1 part in 300 and required about 80 seconds. (This procedure is equivalent to using

██████████



Eq. (1.6) as the C-J condition. While this is incorrect, the resulting error is small as was pointed out in the footnote to that equation.)

4.4 Internal Consistency

Several checks were made on the internal consistency of the calculations in the case of 65/35 RDX/TNT, and the Chapman-Jouguet point (determined as described in the preceding section as the Hugoniot point having minimum D) was found to possess all the properties described in Chapter 1:

(a) The entropy along the Hugoniot is a minimum at the Chapman-Jouguet point to better than five significant figures, and the C-J adiabat lies always below the Hugoniot but above the straight line $(p_o, v_o) \rightarrow (p_{CJ}, v_{CJ})$.

(b) The shock curve for the detonation products originating at the C-J point lies always between the detonation Hugoniot and the C-J adiabat (cf. Table 7.1); thus all three curves are tangent to the line $(p_o, v_o) \rightarrow (p_{CJ}, v_{CJ})$ at the C-J point.

(c) The value of γ^* for the C-J point (determined from (1.5) by numerical differentiation of (p, v) data for the C-J adiabat) together with the calculated value of D_{CJ} gives values of C-J volume and pressure from (1.7) which agree with the directly calculated values to five significant figures.

(d) The value of α^* for the C-J point (determined from (1.8) by numerical differentiation of (e, v) data for the C-J isobar) together





with the calculated value of $d \ln D_{CJ} / d \ln \rho_0$ gives from (1.9) a value of δ^* which agrees with the adiabatic slope to five significant figures.



Chapter 5

EQUATION-OF-STATE PARAMETER STUDIES

The gaseous-equation-of-state constants α , β , χ , and k_i are to be considered as parameters whose values are to be determined empirically to give the best possible agreement with the available experimental data -- principally the variation of detonation velocity (D_{CJ}) with loading density (ρ_0). On this basis, Brinkley and Wilson⁽²⁾ chose the values $\alpha = 0.25$ and $\beta = 0.30$, assuming the volume of solid carbon to have the constant value $V_s = 5.34$ cc/mole (its value at room temperature and 1 atm pressure). They used the set of values of the covolume constants k_i given in Table II.1, which were chosen to give the best possible fit of $D_{CJ} - \rho_0$ curves for a number of different explosives using the same set of parameter values for all explosives. Christian and Snay,⁽⁷⁾ using the above values of α and β followed the same procedure for a much greater variety of explosives (using, however, fixed compositions of the reaction products), and arrived at a considerably different set of covolume constants (also given in Table II.1). Neither set of values appeared too satisfactory to us: the Christian-Snay value for the H_2 covolume is quite small, and among the Brinkley-Wilson values it is surprising to find OH and H_2O having values which are not only equal but also appreciably less than that for H_2 , and to find NO with a value much less than those



for CO, N₂, and O₂.

We have, therefore, calculated a set of covolumes of our own which are primarily geometrical in nature (except that fairly small corrections were applied in the case of the polar molecules H₂O, NO, OH, and NH₃); these values are also given in Table II.1, and details of the manner in which they were calculated are given in Appendix II. Although we have departed somewhat from the geometrical values for reasons discussed in Chapter 6, we still feel the geometrical basis to be of value in providing a means of calculating a covolume for any new molecule which one might wish to include in his list of reaction products.

Although the calculated $D_{CJ} - \rho_0$ curve is rather insensitive to the relative values of the covolumes, it is quite sensitive to the values of β and K used; in addition, the value of α has a sizeable effect on the calculated C-J pressure for a given ρ_0 . As a result of the parameter studies to be described, we have found it desirable to depart drastically from the values $\alpha = 0.25$ and $\beta = 0.30$ used by the other authors.

Except as specifically noted below, these parameter studies were made for 65/35 RDX/TNT (by weight) using the geometrical covolumes given in Table II.1 and the carbon equation of state (2.5). Some preliminary calculations showed that the calculated $D_{CJ} - \rho_0$ curve was essentially the same for equilibrium composition of the reaction products as for a composition held fixed throughout, so that fixed composition was used because of the great saving in time which



[REDACTED]

resulted.^(a) (The fixed composition used was the so-called H₂O-arbitrary composition, which for oxygen-deficient explosives is as follows: all nitrogen is present as N₂, all hydrogen present occurs as H₂O, the remaining oxygen occurs as CO, and the remaining carbon as graphite.) For comparison purposes, the figures to be described include an experimental curve (see Chapter 6) assumed to be represented by the relation

$$D_{CJ} = 3127 \rho_0 + 2673 \text{ m/sec.}$$

Figure 5.1 shows the effect of varying the covolume-scale-factor χ . This effect may be summarized roughly as producing a rotation of the calculated $D_{CJ} - \rho_0$ curve about a point on the ordinate axis, with little change in the shape of the curve. The effect of varying β is shown in Fig. 5.2; decreasing β is seen not only to drop the calculated curve as a whole, but also to decrease the curvature.

The effect of β compared with that of χ is about what one would expect, since in the equation-of-state imperfection factor $F = 1 + x e^{\beta x}$, ($x \propto \chi$), χ affects both x and $e^{\beta x}$ whereas β affects only the latter, which becomes most important at high loading densities. It is evident that different sets of values of β and χ , all of which result in the same calculated value of D at one given

^(a) With fixed composition, the values of k_i used are immaterial.

[REDACTED]

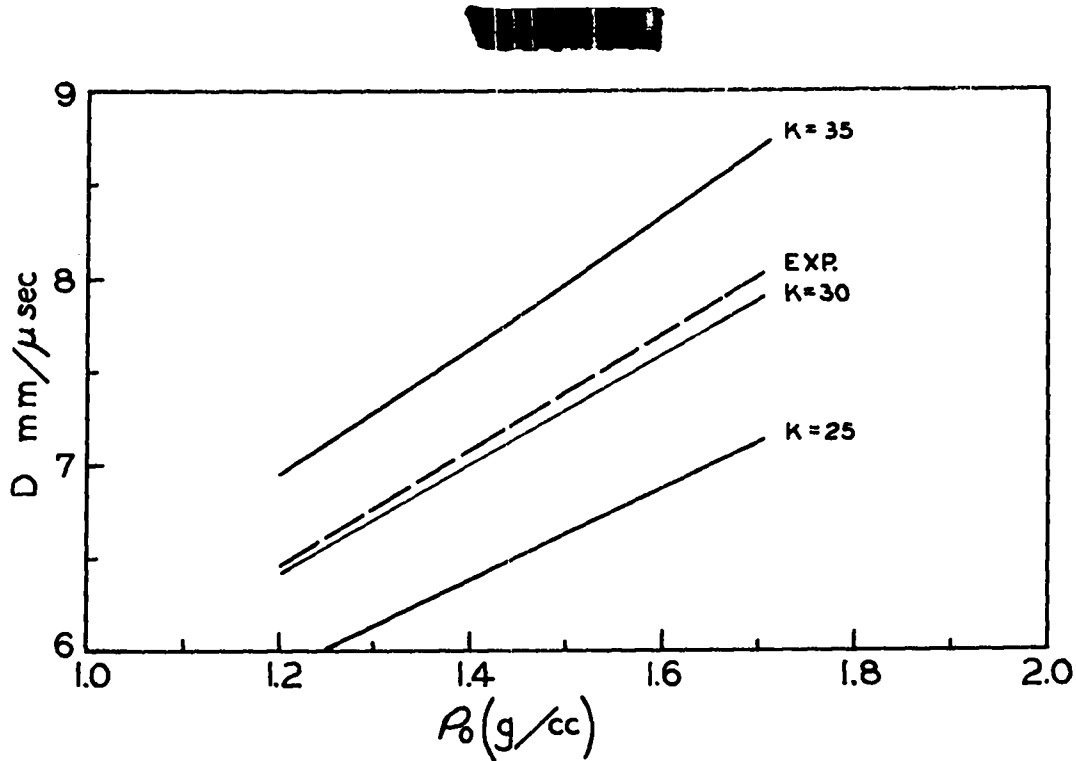


Fig. 5.1 The effect of κ on $D - \rho_0$; $\alpha = 0.6$, $\beta = 0.06$.

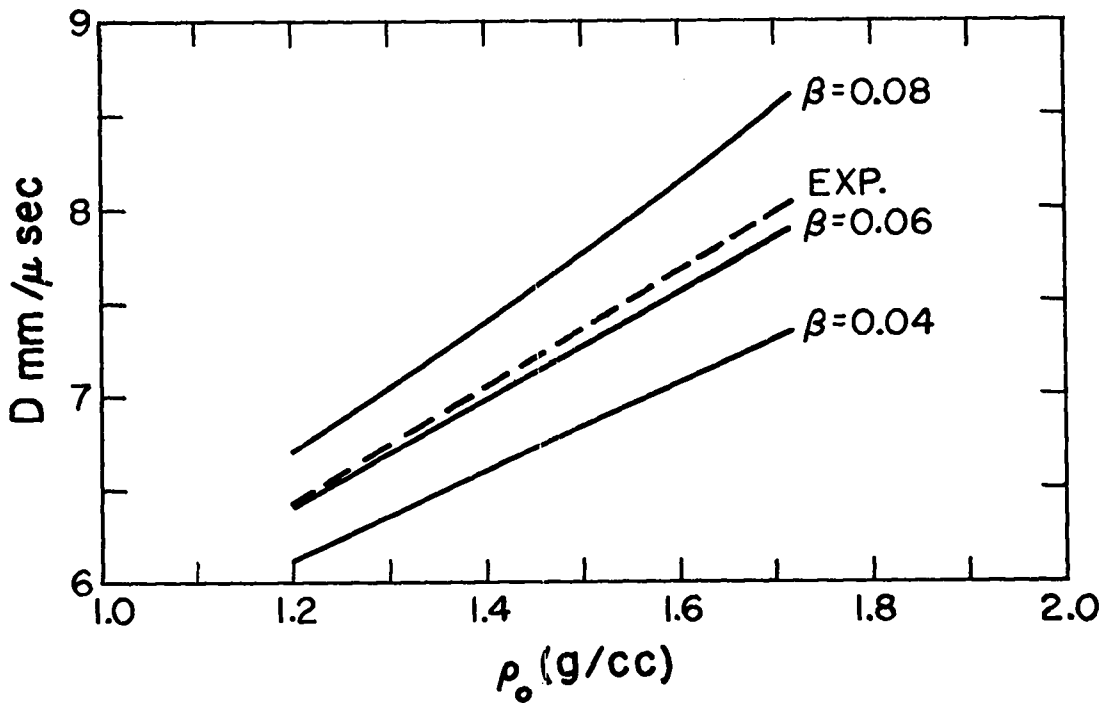


Fig. 5.2 The effect of β on $D - \rho_0$; $\alpha = 0.6$, $\kappa = 30$.

SECRET

loading density, will result in $D - \rho_0$ curves having different average slopes. This is illustrated better in Fig. 5.3, which compares curves for two values of β , with χ determined in each case so as to give the experimental value of D at $\rho_0 = 1.715$ g/cc.

It may be seen from the figures just described that (for 65/35 RDX/TNT, at least) a value of β much less than 0.30 is required to give a good fit to the experimental data. Although the curves shown are for $\alpha = 0.6$, similar curves run for $\alpha = 0.25$ also indicate the value $\beta = 0.30$ to be much too high. The effect of α on the calculated $D_{CJ} - \rho_0$ curve is, in fact, relatively small (provided, of course, that χ is increased with α so as to keep $\chi / (T + \theta)^\alpha$ of constant magnitude).

The important effects of α are shown in Figs. 5.4 and 5.5, which give the results for a series of runs in which β and χ were adjusted for each α to give the best fit to the experimental $D_{CJ} - \rho_0$ curve. Figure 5.4 shows the variation with ρ_0 of the C-J pressure and temperature for three values of α . It may be noted that for large α , T_{CJ} decreases strongly with increasing ρ_0 . Although there are no accurate experimental values of temperature with which to compare these results, such a decrease is not unreasonable since at the high densities a larger fraction of the available energy may be expected to go into imperfection (potential) energy as opposed to

SECRET

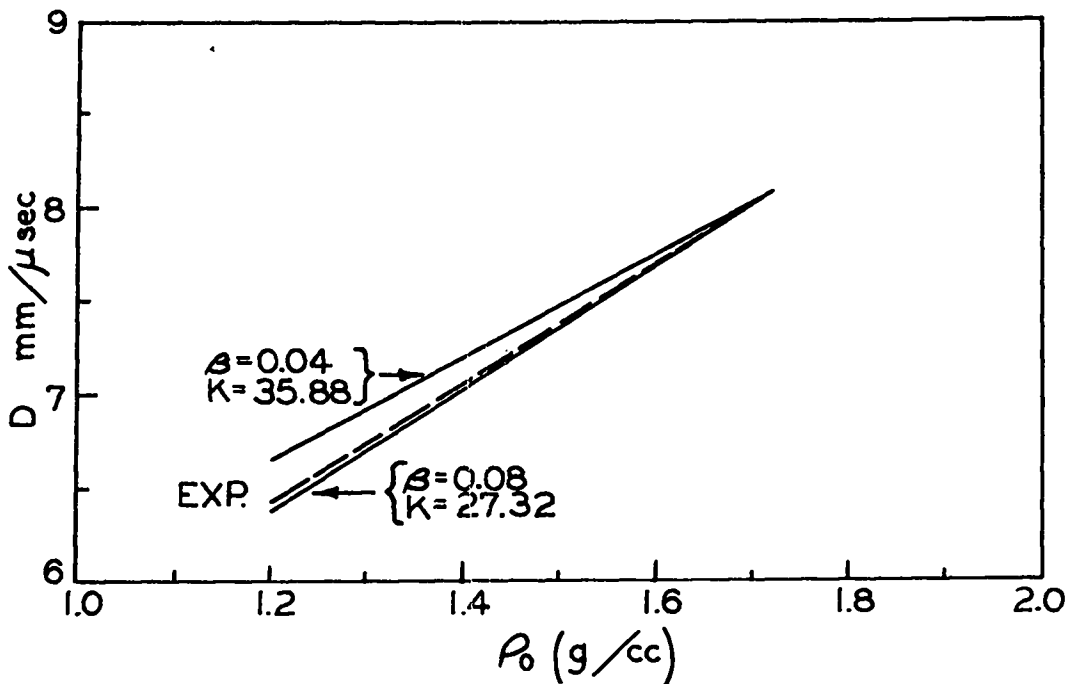


Fig. 5.3 The effect of β on $D - \rho_0$; $\alpha = 0.6$, χ chosen to match experimental D at one point.

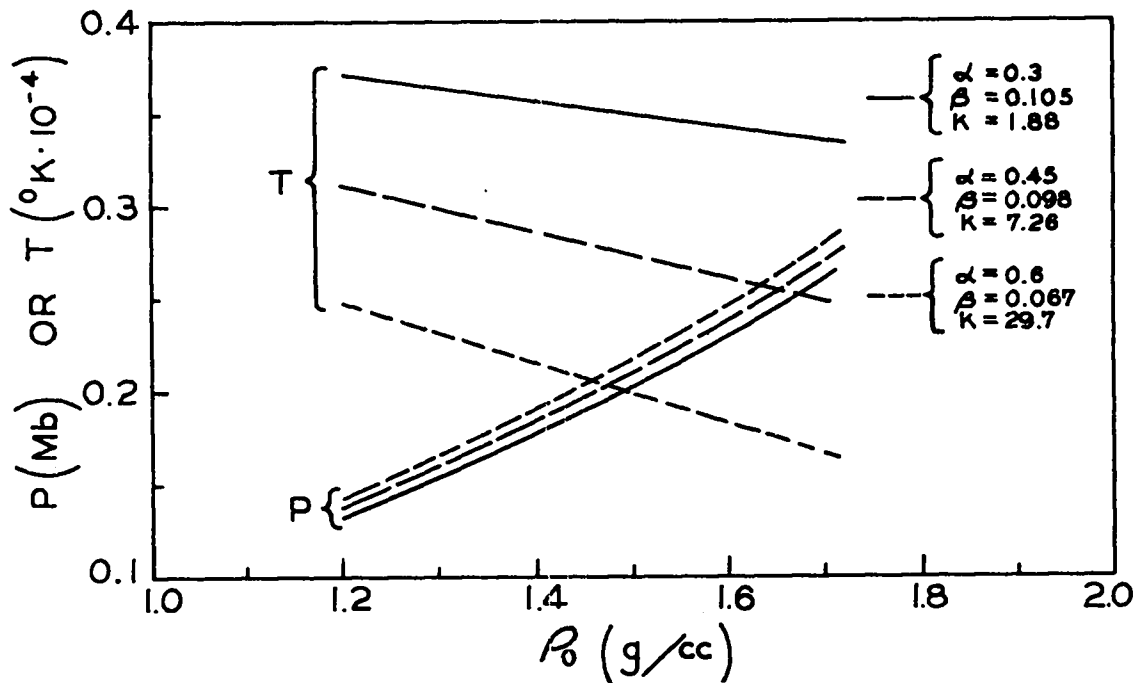


Fig. 5.4 The effect of α on p vs. ρ_0 and T vs. ρ_0 ; β and χ chosen to match experimental $D - \rho_0$.

kinetic energy.^(a) Thus the calculated dependence of temperature on ρ_0 does not provide any argument against the use of values of α greater than 0.25. Figure 5.5 shows the effect of α on the calculated C-J pressure at $\rho_0 = 1.715$ g/cc. As will be discussed in detail in Chapter 6, accurate experimental values of pressure are available, and for 65/35 RDX/TNT a value $\alpha = 0.5$ gives much better agreement with experiment than does $\alpha = 0.25$.

Figure 5.6 shows shock Hugoniots through the C-J point for two values of α . These results are for TNT, with equilibrium composition, the carbon equation of state (2.6), and the least-square k_1 described in Chapter 6. It can be seen that the choice of α has a considerably larger effect on the pressure at small volumes than on p_{CJ} .

There is one serious difficulty associated with the use of values of α greater than 0.25. From Eq. (2.2), the imperfection part of the gas pressure at constant V_g (and neglecting the small effect of composition changes) is proportional to

$$T \times e^{\beta x} \propto \frac{T}{(T + \theta)^\alpha} e^{\frac{\text{constant}}{(T + \theta)^\alpha}}$$

It is evident that for $\theta = 0$, this pressure becomes infinite as T

(a) Independent calculations based on the Lennard-Jones-Devonshire free-volume theory indicate an even stronger decrease in T_{CJ} with increasing ρ_0 .⁽⁴¹⁾

SECRET

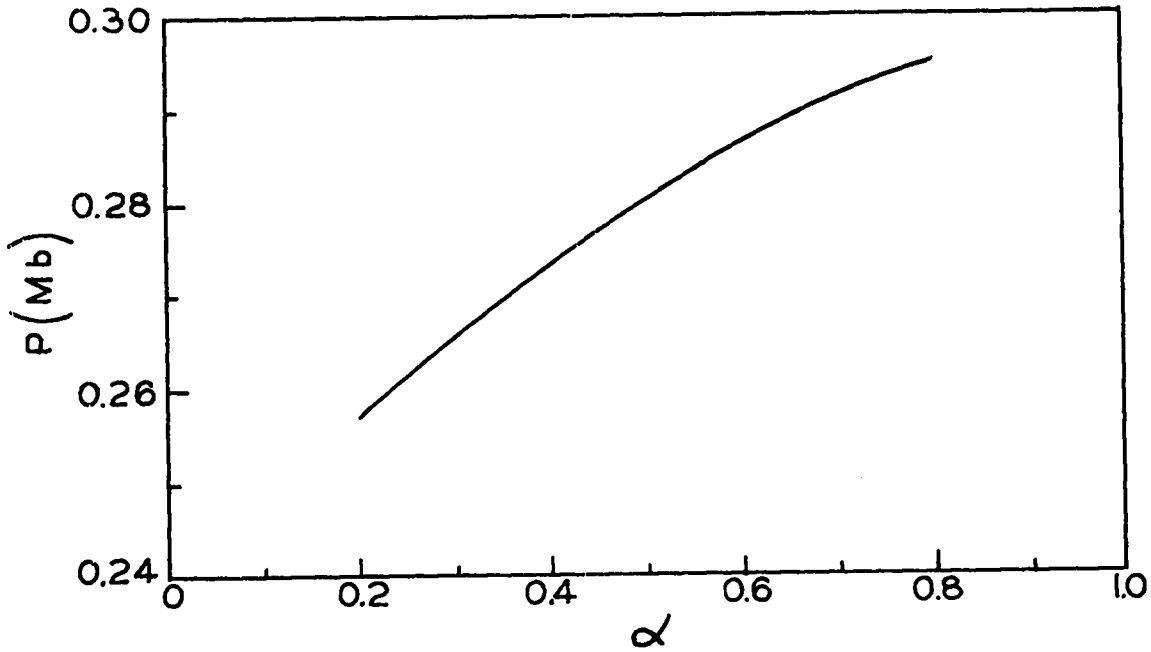


Fig. 5.5 The effect of α on P_{CJ} ($\rho_0 = 1.715$ g/cc); β and κ chosen to match experimental $P_{CJ} \frac{\rho_0}{\rho_0}$.

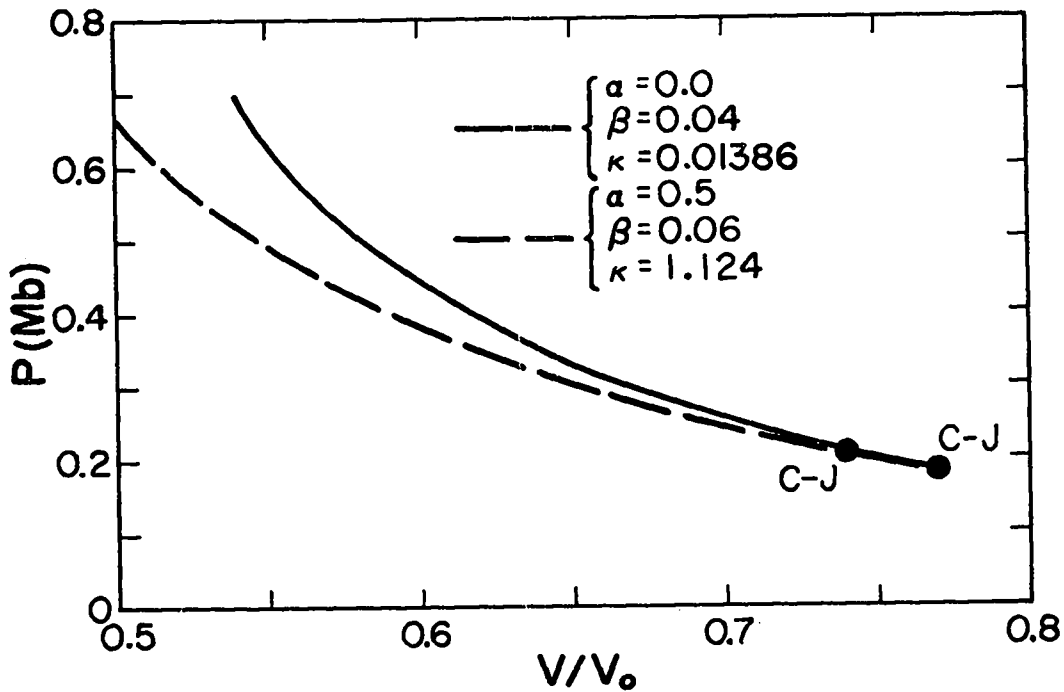


Fig. 5.6. The effect of α on the C-J shock Hugoniot for TNT (see text).

SECRET

tends to zero, and it may in fact be shown that (for $\alpha < 1$) the pressure has a minimum at some temperature T_m . For $\alpha = 0.25$, T_m is of the order of 1°K , so that this feature of the equation of state may safely be ignored. For $\alpha \cong 0.5$, however, T_m becomes 2000°K or more at volumes encountered along the detonation Hugoniot, with serious difficulties resulting. Introduction of the constant θ of course removes the pressure singularity at $T = 0$, but has been only partially effective in removing difficulties with the pressure minimum -- the larger the value of θ used, the more the temperature dependence of x is reduced and consequently the greater the value of α required to match the experimental Chapman-Jouguet pressure. We have settled on the arbitrary value $\theta = 400^\circ\text{K}$ as being large enough to considerably reduce the pressure-minimum difficulties, while still being small compared with all calculated temperatures except those rather far out on the C-J adiabat. With this value of θ , $(\partial p/\partial T)_v$ was always positive for specific volumes greater than about 0.25 cc/g ($v/v_0 > 0.43$ for Composition B, $v/v_0 > 0.48$ for HMX).

The effect of the solid-carbon equation of state on the calculated $D - \rho_0$ curve is shown in Fig. 5.7, which compares results for a fixed molar volume of carbon and for the two equations of state (2.5) and (2.6). All further calculations were made with the equation of state (2.6).

In conclusion, it may be said that for fixed-composition calculations, the values $\alpha = 0.25$ and $\beta = 0.30$ used by Brinkley and

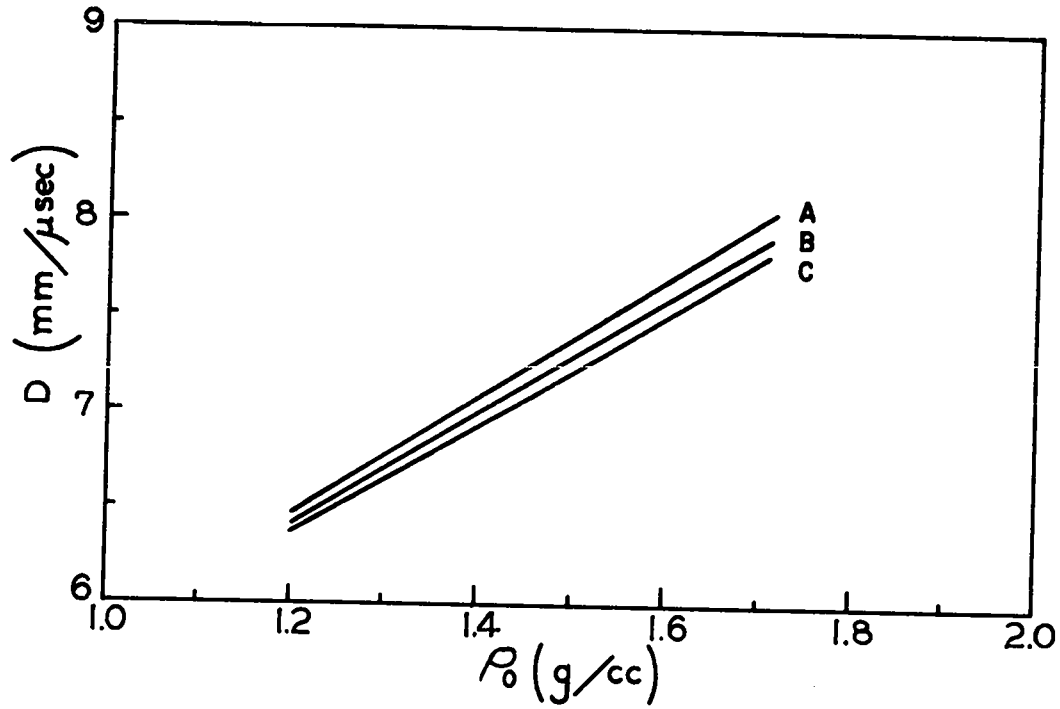


Fig. 5.7 Effect of the graphite equation of state on $D - \rho_0$: A - Incompressible, B - Graphite equation of state used in the parameter studies, C - Graphite equation of state used in the final calculations. All curves are for $\alpha = 0.6$, $\beta = 0.06$, $\eta = 30$.



Wilson and by Christian and Snay appear to need considerable modification, and that $\alpha = 0.6$, $\beta = 0.067$ give much better agreement with experimental data on 65/35 RDX/TNT. For calculations made with equilibrium composition, the situation is qualitatively the same; a detailed discussion is given in the following chapter.



SECRET

Chapter 6

DETERMINATION OF EQUATION-OF-STATE PARAMETERS6.1 Experimental Data

The parameters in the gas equation of state were chosen so as to best match data on D_{CJ} vs. ρ_0 and on p_{CJ} at maximum ρ_0 for a group of five related explosives. These data are summarized in Table 6.1 and were obtained from experimental measurements in the following manner.

Measurements^(a) of the detonation velocity for infinite diameter, D_∞ , were available^(4,5,6) for each explosive at two densities -- $\rho_0 = 1.2$ g/cc, and the highest ρ_0 obtainable by pressing or casting. (Values of D_∞ were obtained by firing charges of different diameter d and extrapolating D vs. $1/d$.) It was assumed on the basis of previous work, both at this laboratory and elsewhere⁽⁸⁾ that over this range of loading density D vs. ρ_0 could be represented by a straight line within experimental error.

The Dural pressures in Table 6.1 were obtained from measurements by GMX-6^(10,39) of shock and free-surface velocities in 24ST Dural plates driven by the appropriate explosives: The particle velocity behind the Dural shock was found from the free-surface velocity with the aid of the graph given by us⁽¹²⁾ and the pressure then calculated

^(a) Accurate to about ± 50 m/sec.

SECRET

TABLE 6.1

Experimental Data for Explosives

Explosive and Density for P_{CJ}	Detonation Velocity ^a $D = A \rho_o + B$, (m/sec)		Dural ^b Pressure (Mb)	C-J Pressure ^c (Mb)
	A	B		
RDX $\rho_o = 1.800$ g/cc	3466	2515	0.398	0.341
90/10 RDX/DNPA ^d $\rho_o = 1.748$	3233	2785	0.378	0.316
78/22 RDX/TNT $\rho_o = 1.755$	3193	2702	0.382	0.317
65/35 RDX/TNT $\rho_o = 1.715$	3127	2673	0.358	(0.286) ^f 0.292
TNT ^e $\rho_o = 1.640$	2799	2360	0.226	0.177

^aFrom data of Refs. 4,5,6.

^dDinitropropylacrylate polymer.

^bFrom data of Ref. 10.

^eMore work on the TNT $D - \rho_o$ curve is in progress.

^cSee text.

^fRef. 11.

SECRET

from the second of Eqs. (1.1).

The explosive C-J pressure was then calculated with the aid of the matching conditions at the HE-metal interface: Letting the subscripts i , r , and t refer respectively to the incident, reflected, and transmitted shocks at the interface, then from (1.1) (taking all velocities in a coordinate system such that $U_{oi} = U_{ot} = 0$ and with the positive direction that of the incident shock)

$$\left. \begin{aligned} p_i &= \rho_{oi} D_i U_i \\ p_t &= \rho_{ot} D_t U_t \end{aligned} \right\} \quad (6.1)$$

$$p_r = p_i + \rho_{or}(U_i - D_r)(U_i - U_r), \quad (6.2)$$

where p_o has been neglected relative to p_i and p_t . Applying the boundary conditions $p_r = p_t$ and $U_r = U_t$, there may readily be derived the well-known relation

$$\frac{p_i}{p_t} = \frac{1 + R(\rho_{oi} D_i / \rho_{ot} D_t)}{1 + R}, \quad (6.3)$$

where from (1.2)

$$R \equiv \frac{\rho_{or}(U_i - D_r)}{\rho_{oi} D_i} = \left\{ \frac{(p_r - p_i)(v_o - v_i)}{(p_i - p_o)(v_i - v_r)} \right\}^{1/2}. \quad (6.4)$$

SECRET

SECRET

Since the shock curve from (p_i, v_i) through (p_r, v_r) is tangent^(a) to the straight line $(p_o, v_o) \rightarrow (p_i, v_i)$ it is evident that $R \cong 1$. The use of this so-called acoustic approximation in (6.3) gives results correct to within a per cent or so; however, we have used values of R obtained by calculating shock curves for the detonation products (cf. Table 7.1).

The measurements of Dural shock and free-surface velocities were made for explosives of slightly differing composition and density, so that before p_{CJ} was calculated as described above the experimental data were first corrected to the composition and density values in Table 6.1 in the following way. From (6.1) and (6.3) with the approximation $R = 1$,

$$\frac{U_t}{U_i} + \frac{p_t}{p_i} = \frac{U_t}{U_i} + \frac{\rho_{ot} D_t U_t}{\rho_{oi} D_i U_i} = 2, \quad (6.5)$$

from which

$$U_t = \frac{2 \rho_{oi} D_i U_i}{\rho_{oi} D_i + \rho_{ot} D_t}. \quad (6.6)$$

Differentiation of (6.6) gives, using (6.6) and (6.5),

$$\frac{\delta U_t}{U_t} = \frac{1}{2} \frac{p_t}{p_i} \left(\frac{\delta \rho_{oi}}{\rho_{oi}} + \frac{\delta D_i}{D_i} - \frac{\delta D_t}{D_t} \right) + \frac{\delta U_i}{U_i}. \quad (6.7)$$

^(a) See the discussion in connection with Eq. (1.4); also Sec. 4.4.

SECRET

CONFIDENTIAL

From (1.1) and (1.7), $U_i = D_i / (\gamma_{CJ}^* + 1)$, so that neglecting the variation of γ_{CJ}^* , $\delta U_i / U_i = \delta D_i / D_i$. Also, from the experimental Hugoniot for Dural⁽³⁹⁾ $\delta D_t / D_t \cong \frac{1}{4} \delta U_t / U_t$. Taking $p_t / p_i \cong 1.22$ and using the experimental dependence of D on composition and density in the neighborhood of 65 RDX/35 TNT (from Table 6.1), Eq. (6.7) can be reduced to

$$\delta U_{fs} / U_{fs} = \delta U_t / U_t = 0.86 \delta \rho_o + 0.0023 \delta (\% \text{ RDX}), \quad (6.8)$$

in which U_{fs} is the experimentally measured free-surface velocity. With the value of U_{fs} thus corrected, the corresponding value of Dural shock velocity was found from the experimental equation of state, and p_t and p_i calculated as previously described. These corrections were of the order of 1 to 3 per cent, and all data in Table 6.1 are believed to be accurate to a per cent or so (including experimental error).

6.2 Determination of α and β

In order to determine a set of equation-of-state parameters from the experimental data of Table 6.1, we started by assuming the set of "geometrical" covolumes described in Appendix II. Using these values of k_1 , the parameters α , β , and χ were varied as described in Chapter 5 so as to give a good match to the experimental data for 65/35 RDX/TNT. The values $\alpha = 0.5$, $\beta = 0.09$, $\chi = 11.8516$ were

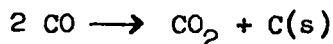
CONFIDENTIAL



found to give results for this explosive agreeing with experiment to about 1% for the $D - \rho_0$ curve and 3% for the C-J pressure; however, the calculated values for the other explosives were quite poor (cf. Fig. 6.1). It would of course have been possible to improve the agreement for the other explosives by choosing a different set of values of α , β , and χ for each explosive. However, it was felt that intercomparison of the equations of state of the various explosives would be more reliable if a single set of values of the parameters could be used for all five; consequently an attempt was made to improve matters by adjusting the covolume values.

6.3 Determination of k_i

An optimum set of values of the k_i (insofar as the $D - \rho_0$ calculations were concerned) was obtained by the following least-square process. From Fig. 7.2 it may be seen that the reaction



shifts markedly to the right as ρ_0 is increased through the range of interest. Because of this strong composition change, points of different ρ_0 for a single explosive were given the same weight in the least-squaring as points for different explosives.

Thus using a guessed set of k_i , a value of $k_{\text{obs}} = \chi \sum x_i k_i$



was determined at four loading densities (1.2, 1.4, 1.6, and maximum) for each of the five explosives by adjusting κ in each case until the calculated D_{CJ} was equal to the experimental value. This gave a set of twenty linear equations for the new set of k_i (corresponding to $\kappa \equiv 1$):

$$\sum_i (x_i)_r k_i = (k_{obs})_r, \quad r = 1, 2, \dots, 20, \quad (6.9)$$

which were then solved by the method of least squares. The first result of this process was large negative values for the H_2 and NO covolumes, presumably because these components are present in mole fractions of only about 10^{-2} to 10^{-5} . Therefore the equations were solved instead with these two covolumes held fixed at their original values (multiplied by the average κ from the determination of all the k_{obs}). Table 6.2 contains the resulting^(a) k_i , together with our

(a) In a preliminary trial of the least-squaring process on three explosives with $\alpha = 0.6$, it was found that carrying out the entire least-squaring process a second time (starting with the k_i produced from the first least-squaring) produced only a small change in the k_i . It was also found that the rather sizeable change in k_i from the initial geometrical set to the first least-square set produced composition changes of at most a few per cent of the original mole fractions. Since the determination of so many k_{obs} is rather expensive in machine time, the final least-squaring was started with the k_i from this trial run and was done only once.



"geometrical" set and the values obtained by Brinkley and Wilson and by Christian and Snay. The changes which the least-squaring process

Table 6.2

Comparison of Covolume Constants

Source	$\frac{k_1}{CO}$					
	H ₂	CO ₂	CO	H ₂ O	N ₂	NO
Brinkley-Wilson ⁽²⁾	153	687	386	108	353	233
Christian-Snay ⁽⁷⁾	60	525	313	285	334	---
"Geometrical"	^a 180	670	390	360	380	350
	^b 2133	7940	4622	4267	4504	4148
Least-square	2133	6407	3383	3636	6267	4148

^aOriginal set, scaled so that k_{CO} would be about the same as that used by Brinkley and Wilson.

^bScaled by the average $K (= 11.8516)$ from the determination of all the k_{obs} (see text).

produced (namely 20 to 25% decreases in the CO₂ and CO covolumes and a 40% increase in the N₂ covolume) are qualitatively what one would expect in order that the calculated $D - \rho_0$ curve for TNT (C₇H₅N₃O₆) should be lowered compared with that for RDX (C₃H₆N₆O₆). However, the fact that the resulting value for k_{N_2} is nearly twice as large as k_{CO} and almost as large as k_{CO_2} indicates that a priori estimation of covolumes on a geometrical basis is rather



unsatisfactory for this equation of state.^(a)

In Figs. 6.1 and 6.2 the calculated results for $D - \rho_0$ are compared with experiment for the geometrical and the least-square covolumes, respectively. (To avoid confusion, results for only three explosives are shown; the others show qualitatively similar effects.) It can be seen that with the least-square k_i fairly good agreement is obtained for all explosives in the case of $D - \rho_0$, and the values of the parameters thus determined are

$$\left. \begin{aligned} \alpha &= 0.50 \\ \beta &= 0.09 \\ \chi &= 1.00 \\ k_i &= \text{least-square set, Table 6.2.} \\ \theta &= 400^\circ\text{K} \end{aligned} \right\} (6.10)$$

The C-J pressures calculated with this set of parameters are compared with the experimental values in Table 7.2. These values do not differ significantly from the pressures calculated with the "geometrical" k_i if allowance is made for the differences in the calculated values of D_{CJ} — i.e., there has been less than one per cent change in the value of γ_{CJ}^* indicated by (1.7).

^(a) It is of course possible that at least part of the apparent difficulty with the geometrical covolumes is actually due to an inaccurate equation of state for the solid carbon (cf. Sec. 7.2).

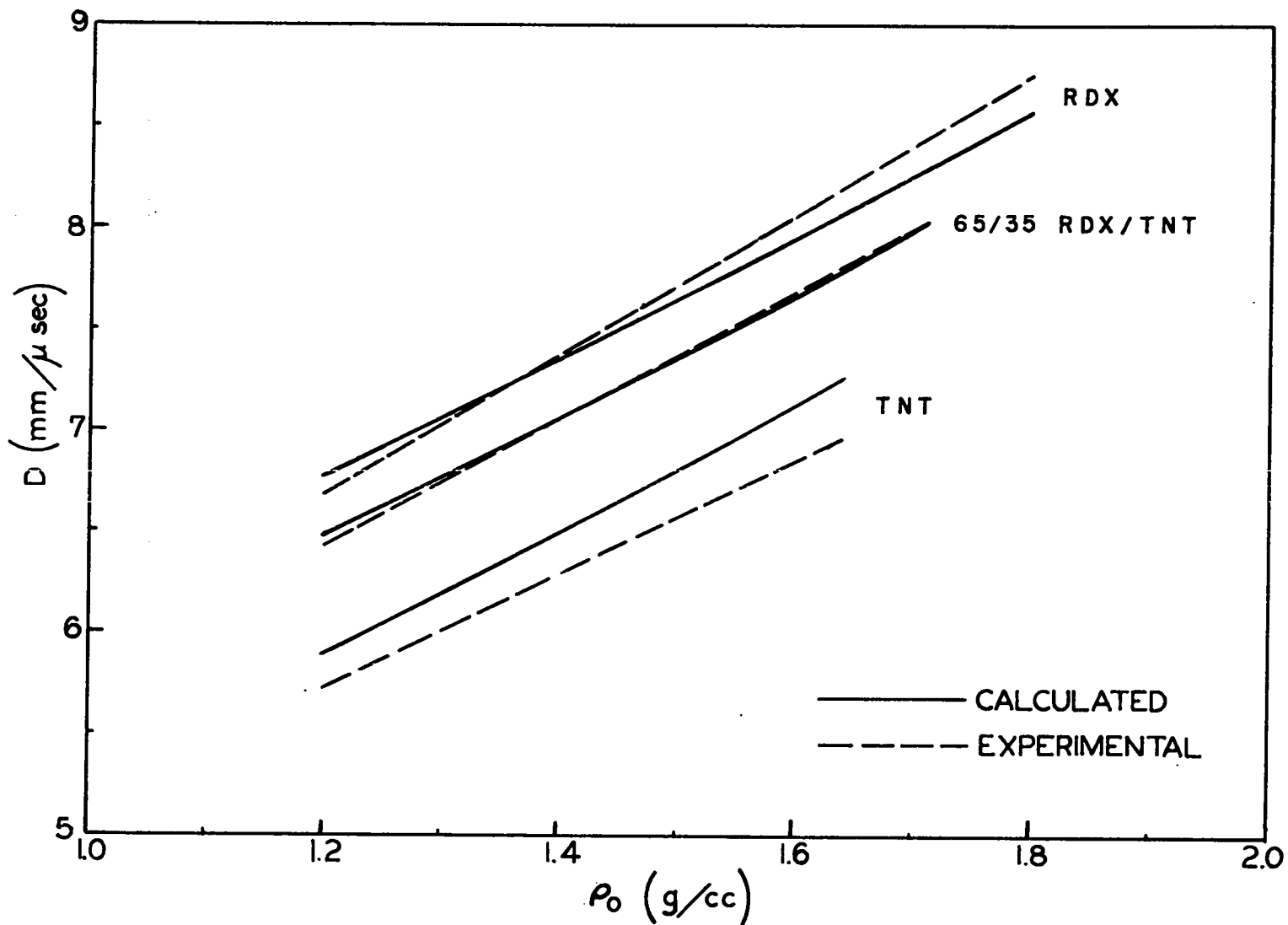


Fig. 6.1 Comparison of calculated and experimental $D - \rho_0$ curves for "geometrical" k_i ; $\alpha = 0.5$, $\beta = 0.09$, $\chi = 11.8516$.

-70-

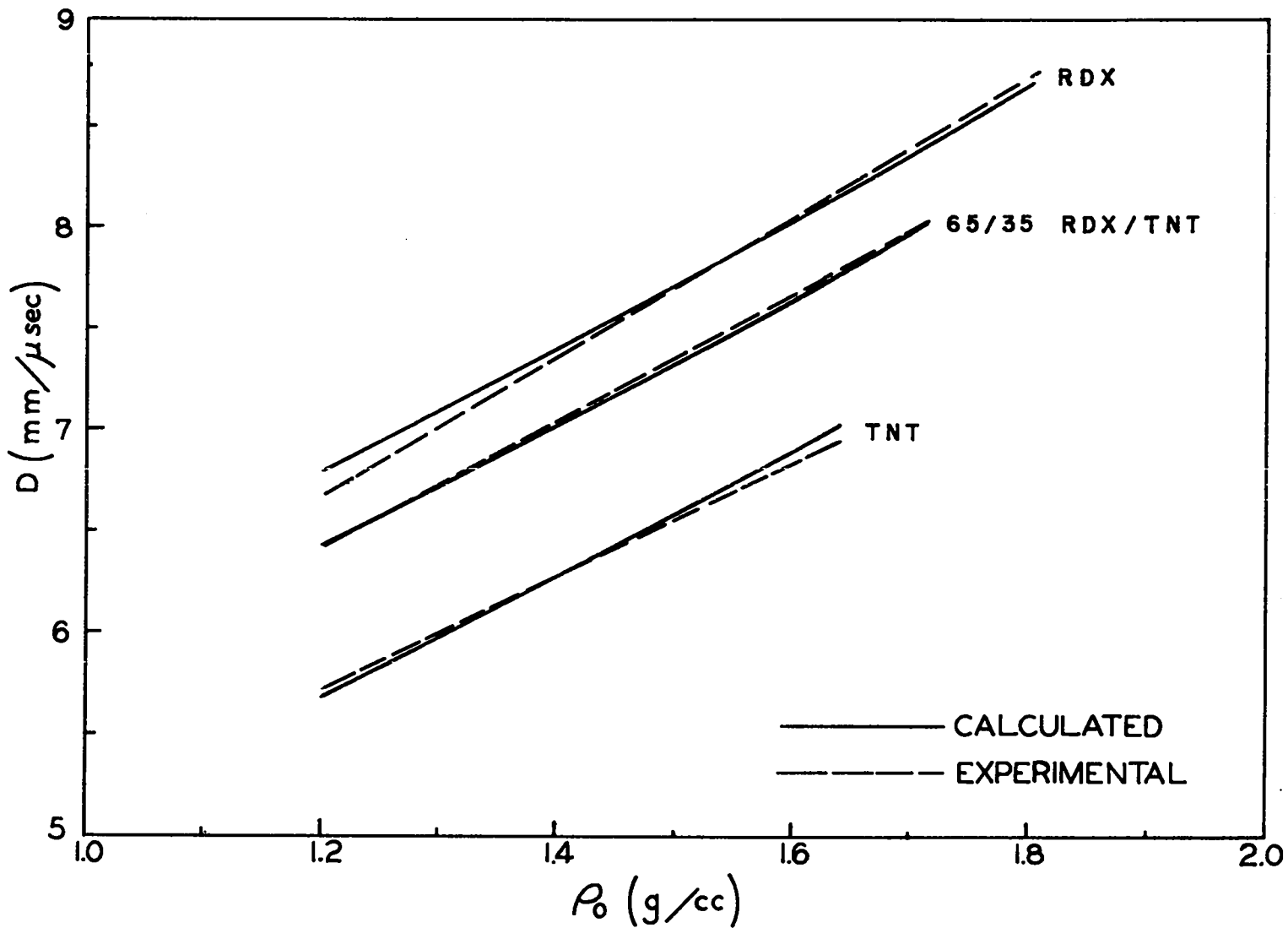


Fig. 6.2 Comparison of calculated and experimental $D - \rho_0$ curves for least-square k_1 ;
 $\alpha = 0.5, \beta = 0.09, \kappa = 1.$

SECRET

Chapter 7

RESULTS7.1 Equation-of-State Data

Calculations of Chapman-Jouguet conditions as a function of loading density for five different explosives are described in Chapter 6, on the basis of which were chosen the values of the gas-equation-of-state parameters given in (6.10). Some of the results of these calculations are given in Fig. 6.2 and Table 7.2. More extensive data (Hugoniot curve, C-J adiabat, and several isocalorics) are tabulated for 65/35 RDX/TNT (Composition B), 77/23 RDX/TNT, 76/24 HMX/TNT, and HMX in Appendix III. The data for HMX even at C-J conditions represent an extrapolation beyond the pressure range for which the equation-of-state parameters were calibrated. No experimental pressure measurements are available, but the calculated value $p_{CJ} = 0.391$ Mb is probably too high by five per cent or more (cf. Table 7.2).

Some results in addition to those in Appendix III are given in Figs. 7.1 through 7.3. Figure 7.1 shows the variation with loading density of the Chapman-Jouguet pressure and temperature for three explosives. The calculated composition of the reaction products of 65/35 RDX/TNT is shown in Fig. 7.2 for C-J conditions as a function of loading density, and in Fig. 7.3 for $\rho_0 = 1.715$ g/cc as a function

SECRET

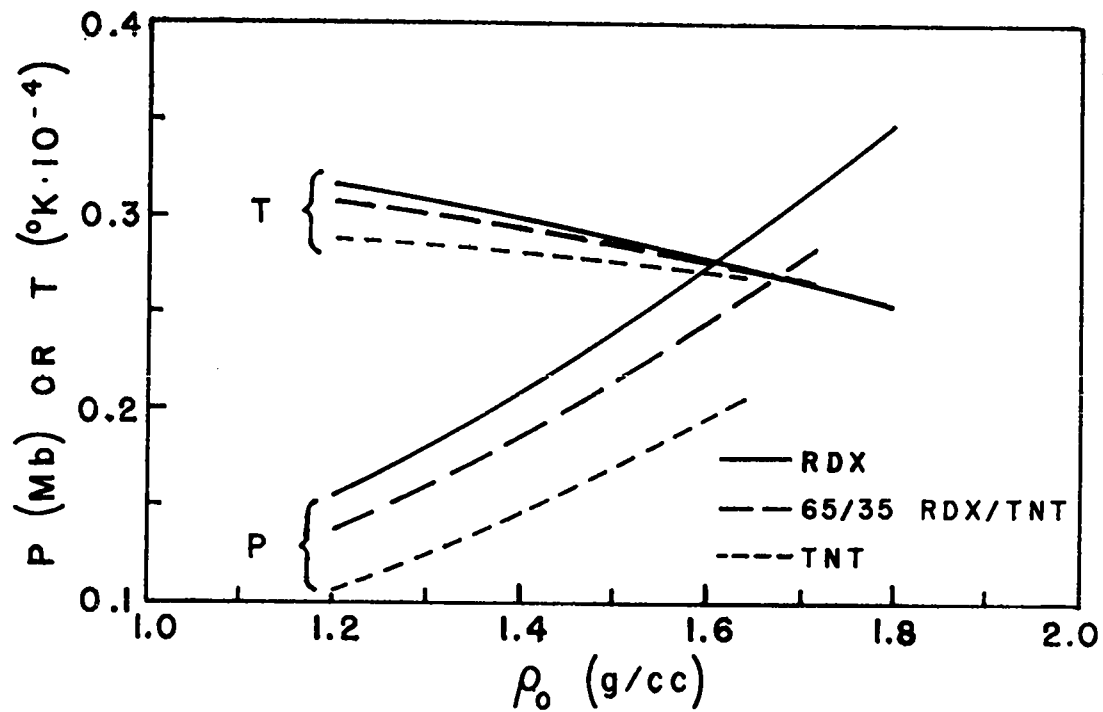


Fig. 7.1 Variation of Chapman-Jouguet pressure and temperature with loading density; Equilibrium composition, $\alpha = 0.5$, $\beta = 0.09$, $\kappa = 1$, least-square k_i .

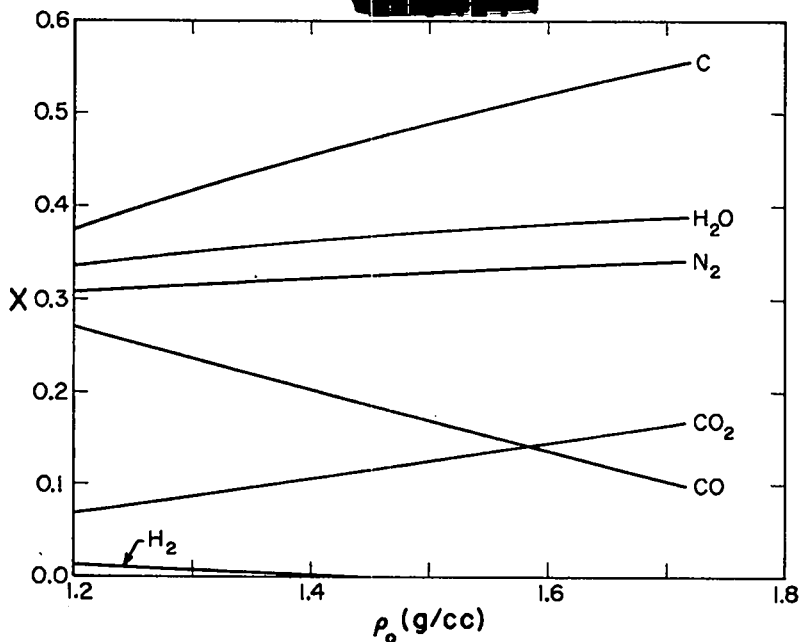


Fig. 7.2 Variation of C-J composition with loading density for 65/35 RDX/TNT. For the gaseous components the ordinate x is the mole fraction n_i/n_g ; for carbon, x is n/N_C , the fraction of the total amount of carbon which is present as graphite.

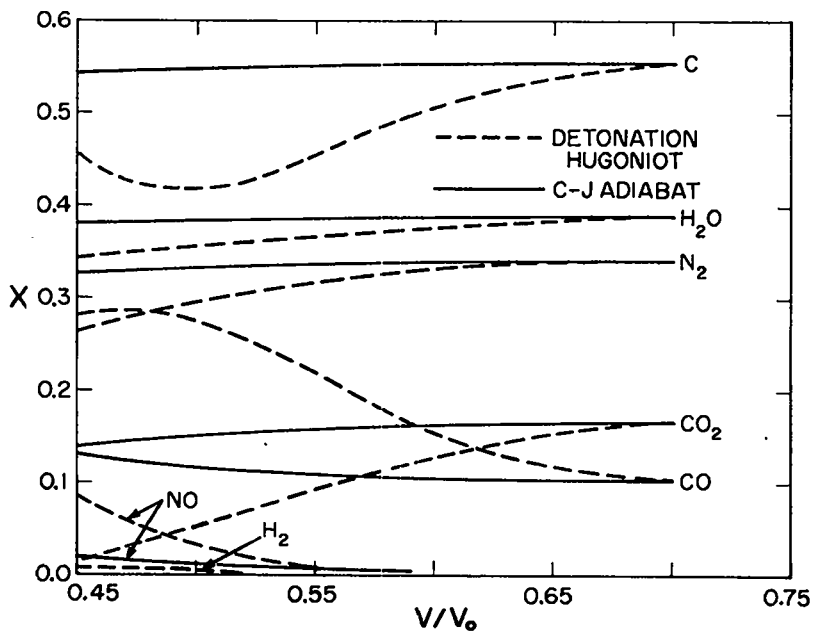


Fig. 7.3 Variation of composition with volume along detonation Hugoniot and C-J adiabat for 65/35 RDX/TNT ($\rho_0 = 1.715$ g/cc)

SECRET

of volume along both detonation Hugoniot and C-J adiabat. The calculated compositions are not necessarily physically meaningful since they depend on the somewhat arbitrary values chosen for the covolumes, k_i ; however, the figures do serve to illustrate the nature of the equilibrium shifts encountered in our calculations. Pressure-volume graphs of Hugoniot and C-J adiabat for 65/35 RDX/TNT are given in Figs. 7.4 and 7.5.

We have calculated the shock curve for shocks traveling into the reaction products of 65/35 RDX/TNT in the C-J state, and these data are given in Table 7.1, together with corresponding data for the C-J adiabat. (In the old CPC implosion calculations carried out by group T-5, reflected shocks back into the HE were approximated with the aid of the appropriate adiabat. As can be seen from the table, the error was negligible.)

7.2 Comparison with Experiment

As was described in detail in Chapter 6, the values of the empirical parameters of the gas equation of state, (6.10), were chosen so as to give good agreement with experiment in the case of D_{CJ} vs. ρ_0 for five explosives, and in the case of p_{CJ} at high loading density for 65/35 RDX/TNT. A comparison of calculation with experiment in the case of $D - \rho_0$ is given in Fig. 6.2, and in the case of D and p at high loading density in Table 7.2. All calculated

SECRET

Table 7.1

Adiabat and Shock Hugoniot Through the C-J Point <u>65/35 RDX/TNT</u>				
v/v_0	<u>Adiabat</u>		<u>Shock Hugoniot</u>	
	p(Mb)	γ^*	p(Mb)	R(Eq. 6.4)
0.600	0.5316	2.98	0.5344	1.259
0.625	0.4710	2.96	0.4723	1.202
0.650	0.4195	2.94	0.4201	1.151
0.675	0.3755	2.93	0.3757	1.104
0.700	0.3377	2.91	0.3377	1.063
0.725	0.3050	2.90	0.3050	1.025
0.743(C-J)	0.2843	2.89	0.2843	1.000
0.750	0.2765	2.89		
0.800	0.2297	2.85		
0.900	0.1646	2.81		
1.000	0.1227	2.76		
1.2	0.0746	2.69		
1.4	0.0495	2.62		
1.6	0.0350	2.55		
1.8	0.0260	2.50		
2.0	0.0201			

Table 7.2

Comparison of Calculated C-J Conditions with Experiment

Explosive, ρ_0 (g/cc)	D_{CJ} (m/sec)		P_{CJ} (Mb)			γ_{CJ}^*		α_{CJ}^*	
	Exp. (a)	Calc.	Exp. (a)	Calc.	Diff.	Exp.	Calc.	Exp.	Calc.
HMX, 1.90		9042		0.3914			2.969		0.287
76/24 HMX/TNT, 1.815		8483		0.3318			2.937		0.281
RDX, 1.80	8754	8702	0.341	0.3488	+2.2%	3.04 ₅	2.908	0.36 ₂	0.293
90/10 RDX/DNPA, 1.748	8436	8444	0.316	0.3194	+1.1%	2.93 ₆	2.901	0.35 ₇	0.290
78/22 RDX/TNT, 1.755	8306	8307	0.317	0.3106	-2.2%	2.81 ₉	2.899	0.28 ₀	0.284
65/35 RDX/TNT, 1.715	8036	8028	0.292	0.2843	-2.8%	2.79 ₃	2.888	0.27 ₅	0.280
TNT, 1.64	6950	7020	0.177	0.2066	+16.6%	3.47 ₅	2.913	0.69 ₅	0.250

(a) Experimental values of D and p are accurate to about ± 50 m/sec and ± 1 or 2%, respectively.



values are in satisfactory agreement with experiment except for the TNT pressure, which is in error by + 17% (of which about 2% is due to the high calculated value of D). The reason for this large disagreement, from the point of view of properties of the equation of state, can be seen better from the quantities γ^* and α^* , which are also given in the table. (a) It is evident that the experimental C-J pressure for TNT corresponds to unusually large values of γ^* and α^* , which the calculations fail to reproduce. The low calculated value of γ^* could be due to several causes: (a) the γ^* given by our graphite equation of state (= 5.65 at the TNT C-J point) is low, (b) the equilibrium equations should predict more carbon to be present, (c) the gas equation of state does not predict sufficiently large changes in γ^* with changes in gas composition, or (d) the gas composition should be different from what it is (probably in the direction of larger components). Which of these causes (if any) is the correct explanation remains at present unknown. It may be said, however, that there is some uncertainty in connection with the experimental $D - \rho_0$ curve for TNT, and experimental work is continuing.

Some preliminary calculations have shown that even if α is reduced to zero, the calculated p_{CJ} for TNT is still a little above the experimental value. This change in α has a marked effect on the

(a) Values of γ^* were calculated from the second of equations (1.7); experimental values of α^* were obtained from (1.9) and values of A in Table 6.1; calculated values of α^* were found from (1.8) by numerical differentiation of data along the appropriate isobars. The different means of determining experimental and calculated values of α^* is of no consequence (see Sec. 4.4).



pressure at smaller volumes (Fig. 5.6). An experiment which might provide some information on this point is the measurement of shock pressures in tuballoy similar to those in Dural which are quoted in Table 6.1. Such experiments are in progress, but results to date are incomplete. It is also uncertain how conclusive the final results will be since an error analysis of the problem of calculating the volume of the HE reaction products is rather unfavorable: Thus suppose that shock measurements in Dural are used to determine the C-J point (as described in Chapter 6) and the tuballoy measurements to then determine a point (p_2, v_2) on the C-J shock curve. Assuming the shock velocities in the metals to be accurately known functions of the corresponding particle velocities, then the uncertainties due to experimental errors in U_D and U_T are roughly (for Composition B)

$$\left\{ \begin{array}{l} \delta p_{CJ}/p_{CJ} = 1.08 \delta U_D/U_D \\ \delta v_{CJ}/v_{CJ} = -0.39 \delta U_D/U_D \end{array} \right.$$

$$\left\{ \begin{array}{l} \delta p_2/p_2 = 1.14 \delta U_T/U_T \\ \delta v_2/v_2 = 0.96 \delta U_T/U_T - 1.47 \delta U_D/U_D \end{array} \right.$$

With probable errors of about 1% each in U_D and U_T , the error in

the calculated value of v_2 is then $\pm 1.8\%$, which means a total uncertainty in v_2 approximately equal to the volume difference between the two curves of Figure 5.6 at the tuballoy pressure of about 0.35 Mb.

7.3 Comparison with Jones-Keller Equation of State

The data for 65/35 RDX/TNT represent an equation of state for Composition B designed to replace the old Jones-Keller equation of state⁽²¹⁾ which has been used for practically all implosion calculations in the past. Figure 7.4 compares the detonation Hugoniot for the two equations of state, and Figure 7.5 shows our C-J adiabat together with the Jones-Keller adiabat which passes through our Chapman-Jouguet point. The large difference between our C-J point ($p = 0.284$ Mb, $v/v_0 = 0.743$) and Keller's ($p = 0.207$ Mb, $v/v_0 = 0.796$) is due in part to the density and composition differences (with the associated difference in detonation velocity), but is largely due to Keller's very large $\gamma_{CJ}^* = 3.90^{(a)}$ (cf. Eqs. 1.7). This value is the result of Jones' high γ_{CJ}^* (3.497 for $\rho_0 = 1.5$ g/cc), which is in turn probably due to too high a slope of his calculated $D_{CJ} - \rho_0$ curve (cf. Eq. 1.9): Jones has not published his curve for Composition B, but his equation of state was the same as that which he used for TNT and his $D - \rho_0$ curve for TNT⁽¹⁹⁾ rises very rapidly at high loading densities, $d \ln D / d \ln \rho_0$ being 1.11 compared with experimental values (from Table 6.1) of about 0.67.

^(a)Reference 21, p. VIII-8.

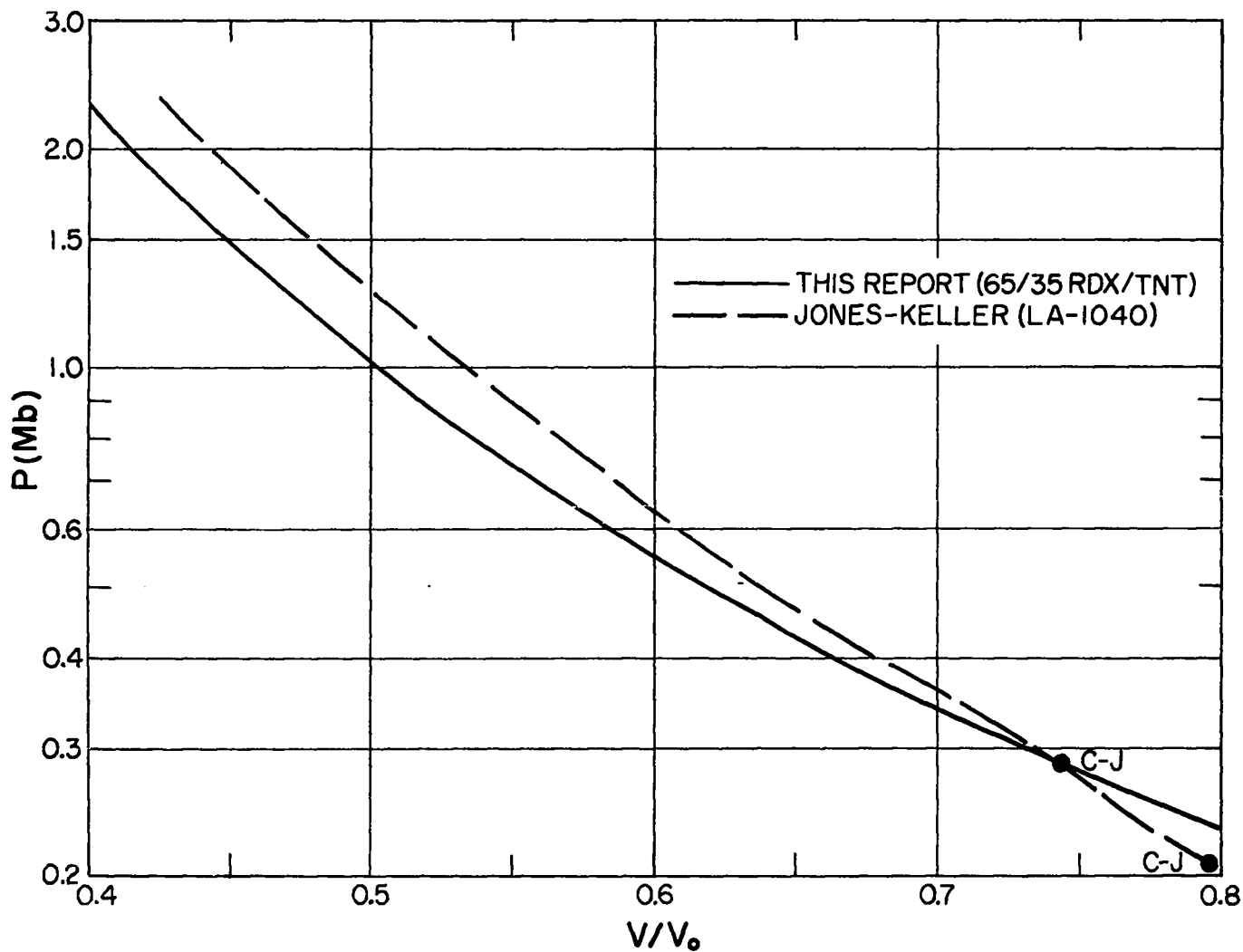


Fig. 7.4 Comparison of theoretical detonation Hugoniot curves. The Jones-Keller curve is for 60/40 RDX/TNT at a loading density of 1.67 g/cc. (Thus the abscissa for the dashed curve is 1.67 v, while the abscissa for the solid curve is 1.715 v.)

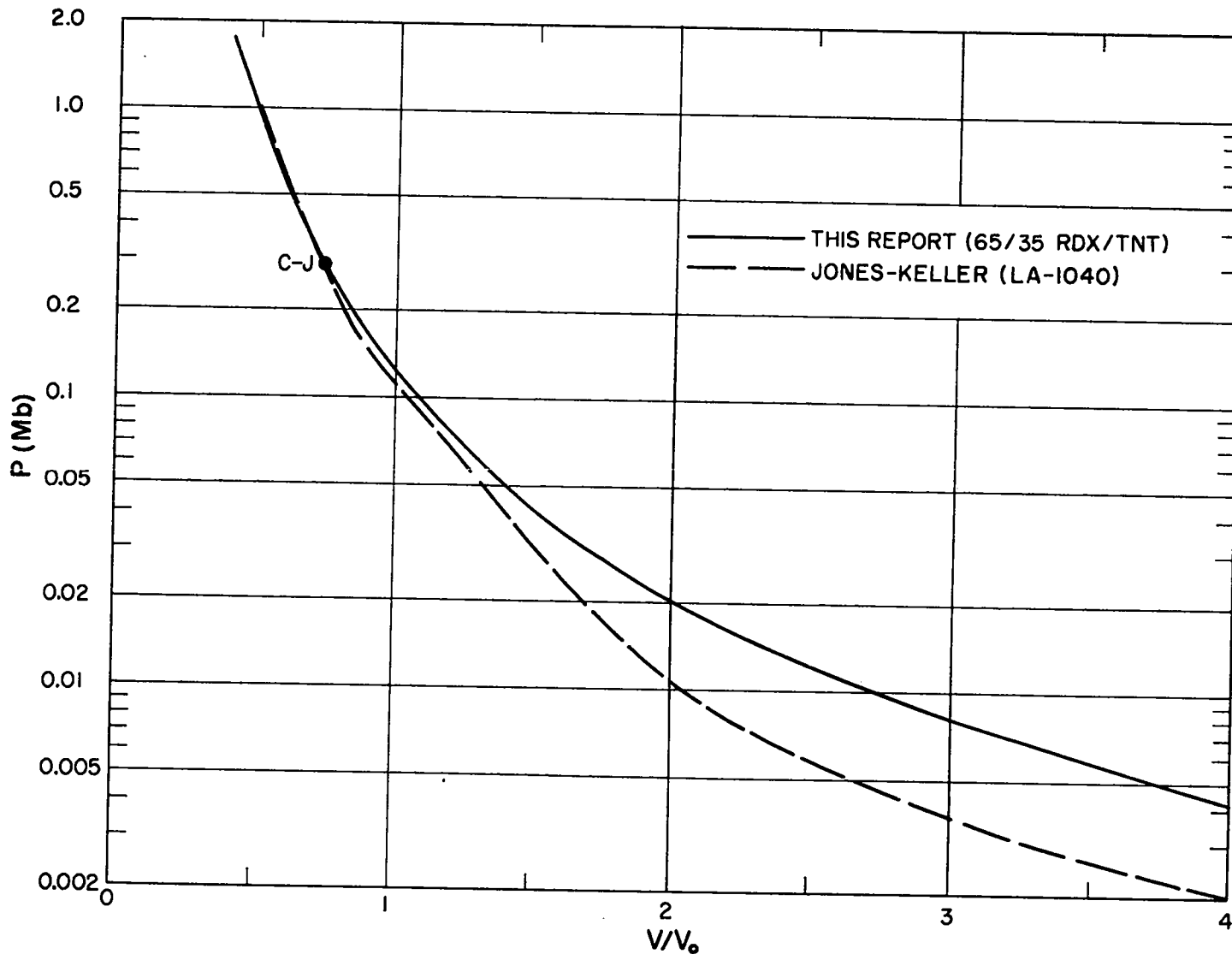


Fig. 7.5 Comparison of Chapman-Jouguet adiabats. (The abscissa for both curves is $v/v_0 = \rho_0 v = 1.715 v$.)



Corresponding to the large difference in the values of γ_{CJ}^* , our Hugoniot curve is much less steep than the Jones-Keller one, and has about a 20% lower pressure at small volumes. Although our Hugoniot curve is certainly nearly correct in the vicinity of its C-J point (since it is tangent to the correct straight line of slope $-\rho_0 D_{CJ}^2$ at about the right point), there is no evidence to indicate whether it has the right curvature and is anywhere near correct at high pressures. Here again a tuballoy plate shot (with Composition B) similar to that discussed in Sec. 7.2 for TNT would probably help to clarify the situation. However, with the same assumptions about the experimental errors, the total uncertainty in the determination of the volume would be about equal to the volume difference of the two curves of Figure 7.4 at the tuballoy pressure of 0.5 Mb.

7.4 Conclusions

One of the purposes of the work here reported was to derive equations of state such that the efficiencies of various high explosives could be compared through implosion calculations to be carried out by group T-5. For purposes of such intercomparison, it is felt that the data of Appendix III should be fairly reliable. As to the absolute accuracy of each equation of state, the situation is less clear. The Kistiakowsky-Wilson equation of state with parameter values given in (6.10) has proved capable of giving satisfactory agreement with experiment





for cyclotols from 65 to 100% RDX in the vicinity of the Chapman-Jouguet point. However, its failure to give good agreement with experiment for pure TNT indicates that it is probably unreliable for an extended extrapolation to explosives of other compositions (unless the parameters are re-evaluated) or even, for a given explosive, to conditions far removed from the C-J point. This is particularly true if the extrapolation is toward smaller volumes, where a minimum in p vs. T will be encountered as discussed in Chapter 5. Because of this and the disagreement with experimental data for TNT, the Kistiakowsky-Wilson equation of state cannot be considered to be entirely satisfactory, and further work may result in its replacement by the Lennard-Jones-Devonshire free-volume equation of state.⁽⁴¹⁾





REFERENCES


1. P. W. Bridgman, "The Compression of 39 Substances to 100,000 kg/cm²," Proc. Am. Acad. Arts. Sci. 76, 55(1948).
2. S. R. Brinkley, Jr., and E. B. Wilson, Jr., "Revised Method of Predicting the Detonation Velocities in Solid Explosives," OSRD-905 (NDRC B-374)(1942).
3. S. R. Brinkley, Jr., and E. B. Wilson, Jr., "Calculation of the Detonation Velocities of Some Pure Explosives," OSRD-1707 (1943).
4. A. W. Campbell, E. James, M. Malin, C. W. Mautz and M. J. Urizar (LASL), unpublished communications.
5. A. W. Campbell, M. Malin, T. J. Boyd and J. A. Hull, "Techniques for the Measurement of Detonation Velocity," Second Symposium on Detonation, Sponsored by Office of Naval Research, Washington, D. C., Feb., 1955.
6. A. W. Campbell, M. Malin and T. Holland, "Detonation in Homogeneous Explosives," Second Symposium on Detonation, Sponsored by Office of Naval Research, Washington, D. C., Feb., 1955.
7. E. A. Christian and H. G. Snay, "Analysis of Experimental Data on Detonation Velocities," NAVORD Report 1508 (1951).
8. N. L. Coleman and T. P. Liddiard, "The Rates of Detonation of Several Pure and Mixed Explosives," NAVORD Report 2611 (1952).
9. R. D. Cowan (LASL), unpublished communication.
10. W. E. Deal, "The Measurement of C-J Pressure in Explosives," Second Symposium on Detonation, Sponsored by Office of Naval Research, Washington, D. C., Feb., 1955.



11. R. E. Duff and E. Houston, "Measurement of C-J Pressure and Reaction Zone Length in a Detonating High Explosive," Second Symposium on Detonation, Sponsored by Office of Naval Research, Washington, D. C., Feb., 1955.
12. W. Fickett and R. D. Cowan, "Free Surface Acceleration by Shocks of Moderate Strength," LA-1568 (1953).
13. W. Fickett and R. D. Cowan, "Values of Thermodynamic Functions to 12,000 °K for Several Substances," LA-1727 (1954).
14. K. Fuchs and T. H. R. Skyrme, "Detonation Waves," LA-1039, Section 6.1 (1948).
15. G. Herzberg, Infrared and Raman Spectra of Polyatomic Molecules (D. Van Nostrand Co., Inc., New York, 1945).
16. G. Herzberg, Spectra of Diatomic Molecules (D. Van Nostrand Co., Inc., New York, Second Edition, 1950).
17. I. Jaffe, R. G. Miller, W. H. Evans and E. J. Prosen, NBS Report 5B110.
18. H. Jones, Third Symposium on Combustion and Flames and Explosion Phenomena (Williams and Wilkins, Baltimore, 1949), pp. 590-594.
19. H. Jones and A. R. Miller, "The Detonation of Solid Explosives: The Equilibrium Conditions in the Detonation Wave-Front and the Adiabatic Expansion of the Products of Detonation," (TNT), Proc. Roy. Soc. (London), A 194, 480-507 (1948). Contained in part in BM-45 (RC-212)(1941).
20. H. Jones and C. A. Strickland, "The Adiabatic Expansion of Detonated 60/40 RDX/TNT with Applications to Fragment Velocities and Shock Wave Pressures," BM-647 (RC-371)(1943).



- 
21. J. Keller, "Equation of State of High Explosives," LA-1040, Chapter 8 (1949). (More detailed equation-of-state tables are available from group T-5.)
 22. J. Keller and N. Metropolis, "Equation of State of Metals," LA-385 (1945).
 23. J. G. Kirkwood, S. R. Brinkley, Jr., and J. M. Richardson, "The Pressure Wave Produced by an Underwater Explosion. Part V," OSRD-2022 (1943).
 24. J. G. Kirkwood and W. W. Wood, "Structure of a Steady-State Plane Detonation Wave," J. Chem. Phys. 22, 1915 (1954).
 25. G. B. Kistiakowsky and E. B. Wilson, Jr., "Final Report on the Hydrodynamic Theory of Detonation and Shock Waves," OSRD-114 (1941).'
 26. H. G. Kolsky and G. N. White, Jr., "The IBM Equation of State for 75/25 Cyclotol and the New Explosive Problem (E-1)," LA-1248 (1951).
 27. N. Metropolis, "Equations of State and Associated Shock-Wave Variables for Certain Metals," LA-208 (1945).
 28. W. E. Milne, Numerical Calculus (Princeton University Press, Princeton, N. J., 1949), pp. 36 ff.
 29. L. Pauling, The Nature of the Chemical Bond (Cornell University Press, Ithaca, New York, 2nd ed., 1940), p. 189.
 30. A. Popolato (LASL), private communication.
 31. E. J. Prosen (NBS), private communication.
 32. cf. J. R. Reitz, "The Nuclear Contribution to the Equation of State of Metals," LA-1454 (1952).

- 
33. F. D. Rossini, Chemical Thermodynamics (John Wiley & Sons, Inc., New York, 1950).
 34. L. Sitney (LASL), unpublished communication.
 35. H. G. Snay and I. Stegun, "Auxiliary Functions for Thermodynamic Calculations Based on the Kistiakowsky-Wilson Equation of State," NAVORD Report 1732 (1951).
 36. G. Stegeman, "Heat of Combustion of Explosive Substances," OSRD-5306 (1945).
 37. H. S. Taylor and S. Glasstone, A Treatise on Physical Chemistry Vol. II, States of Matter (D. Van Nostrand Co., Inc., New York, Third edition, 1951), p. 301, pp. 328-338.
 38. U. S. National Bureau of Standards, "Selected Values of Chemical Thermodynamic Properties, Series III," (loose leaf).
 39. J. M. Walsh and R. H. Christian, "Equation of State of Metals from Shock Wave Measurements," Phys. Rev., in press.
 40. J. M. Walsh and F. L. Yarger (LASL), unpublished communication.
 41. W. W. Wood and W. Fickett (LASL), private communication.

Appendix I

SOLUTION OF THE EQUILIBRIUM EQUATIONS

We have solved the equilibrium equations described in Sec. 4.2 in the following way.

Case (1) - Solid Carbon Present

Letting

$$\left. \begin{aligned} K'_1 &= K_1 K_2 K_3 = \frac{n_6}{n_3 n_5^{1/2}} \\ K'_2 &= K_1 K_2 = \frac{n_3 n_6}{n_2 n_5^{1/2}}, \\ K'_3 &= K_1 K_3 = \frac{n_4}{n_1 n_3}, \end{aligned} \right\} \quad (I.1)$$

these expressions and the equilibrium Eqs. (4.4) and (4.6) can be readily combined to give the equations

$$2 n_5 + K'_1 n_3 n_5^{1/2} - N_N = 0 \quad (I.2)$$

$$n_4 \left(1 + \frac{n_1}{n_4} \right) = n_4 \left(1 + \frac{1}{K'_3 n_3} \right) = \frac{N_H}{2} \quad (I.3)$$

$$2 K_3 n_3^2 + \left(1 + K'_1 n_5^{1/2} \right) n_3 - \left(N_0 - \frac{N_H K'_1 n_3^{1/2}}{K'_3 n_3 + 1} \right) = 0 \quad (I.4)$$



These equations were solved by the following method: (a) Guessing a value of n_3 , (b) solving (I.2) for $n_5^{1/2}$, (c) solving (I.4) as a quadratic in n_3 , (d) iterating steps (b) and (c) till the calculated value of n_3 became constant (using "linear feedback"⁽²⁸⁾), and finally, (e) calculating n_4 from (I.3) and the remaining mole numbers from (4.4) and (4.6).

Case (2) - No solid Carbon Present

Deleting n_7 from (4.4) and ignoring the equation involving K_3 in (4.6), the remaining six equations can be combined to give:

$$2 n_5 + \frac{K_2(N_H - 2 n_1)}{2 n_1} n_5^{1/2} - N_N = 0 \quad (\text{I.5})$$

$$n_2 = \frac{N_C}{1 + K_1(n_1/n_4)} \quad (\text{I.6})$$

$$\left\{ \begin{array}{l} \frac{N_C}{1 + K_1(n_1/n_4)} + n_4 + K_2 n_5^{1/2} (n_4/n_1) = N_0 - N_C \\ \text{or} \\ \left\{ K_1(N_0 - N_C) \right\} (n_1/n_4)^2 - \left\{ 2 N_C - N_0 + N_H/2 + (K_1 - 1)n_1 + K_2 n_5^{1/2} \right\} (n_1/n_4) \\ - K_2 n_5^{1/2} = 0 \end{array} \right. \quad (\text{I.7})$$





$$n_1 = \left(\frac{N_H}{2} \right) \frac{(n_1/n_4)}{1 + (n_1/n_4)} \quad (I.8)$$

These equations were solved by: (a) Guessing a value of n_1 , (b) solving (I.5) for $n_5^{1/2}$, (c) solving (I.7) as a quadratic in n_1/n_4 , (d) calculating a new n_1 from (I.8), (e) iterating steps (b)-(d) (with linear feedback on n_1) until the value of n_1 became constant, and finally (f) calculating n_2 from (I.6) and the remaining mole numbers from (4.4).



Appendix II

CALCULATION OF GEOMETRICAL COVOLUMES

The covolumes used by Brinkley and Wilson⁽²⁾ and by Christian and Snay,⁽⁷⁾ obtained by the curve-fitting procedures mentioned in Chapter 5, are given in Table II.1 in this appendix. In the last column of this table are listed the "geometrical" covolumes which we used for our preliminary calculations; these values were determined on the basis of the following considerations.

Strictly geometrical values were calculated using internuclear distances and angles from Herzberg^(15,16) and the following Van der Waals atomic radii:

$$\left. \begin{aligned} r_H &= 1.20 \text{ \AA} \\ r_C &= 1.60 \\ r_N &= 1.50 \\ r_O &= 1.40 \end{aligned} \right\} \quad (\text{II.1})$$

The radii for hydrogen, nitrogen, and oxygen were taken from Pauling.⁽²⁹⁾ The value for carbon (since Pauling gives none) was simply assumed to be 1.60 to make the C-N-O progression arithmetic (however, it may be noted that the interplanar distance in graphite is 3.40 Å, indicating $r_C \leq 1.70 \text{ \AA}$). There arises the question whether to calculate an actual volume of the non-rotating molecule, or a volume of the rotating

molecule represented as a sphere whose radius is the maximum dimension of the molecule measured from its center of mass. There is some reason to expect that rotational motion might be inhibited at the high densities of interest here. However, there is no clear-cut evidence on this question, and since the high densities on the Hugoniot curve are accompanied by high temperatures which tend to maintain the rotation, we have assumed the rotating-molecule model. (This is consistent with the way in which thermodynamic data were used in our calculations, the thermodynamic functions all being considered as though full thermal rotation existed.)

Covolumes calculated on this basis for the molecules of interest are given in the third column of Table II.1, and are related to the volume V_i of the rotating molecule as follows:

$$k_i = 10.46 V_i, \quad (\text{II.2})$$

where V_i is in \AA^3 , and the factor 10.46 was introduced to make the covolume for CO the same as the Brinkley-Wilson value for easier comparison. Corrections were applied to these values in the cases of polar molecules by means of the following rough considerations.

The Van der Waals potential energy of interaction between two like non-polar molecules a distance r apart may be represented by the Lennard-Jones expression

$$U(r) = \epsilon \left(\frac{r_0}{r} \right)^{12} - 2\epsilon \left(\frac{r_0}{r} \right)^6,$$


where we may take as a measure of the diameter of either molecule the constant r_0 , which is the separation r at which the potential is a minimum. In the case of a polar molecule, there are added to the energy two additional terms of the form $-(I + O) \left(\frac{r_0}{r} \right)^6$, where the constant I represents the effect of interactions between the permanent dipole of one molecule and an induced dipole in the other, and the constant O represents the average interaction between permanent dipoles. This last effect depends on the relative orientation of the molecules, and for a Boltzman distribution of orientations O is inversely proportional to the temperature. The average separation r'_0 of the molecules at the potential minimum is then given by

$$\left(\frac{dU'}{dr} \right)_{r=r'_0} = 12\epsilon \left(\frac{r_0}{r'_0} \right)^{11} - 6(2\epsilon + I + O) \left(\frac{r_0}{r'_0} \right)^5 = 0,$$

or

$$\left(\frac{r_0}{r'_0} \right)^6 = \frac{2\epsilon + I + O}{2\epsilon}.$$

Assuming that r'_0 and r_0 are, respectively, measures of the molecular diameters with and without dipole effects, we then find



 5110


$$\frac{(k_i)_{\text{corrected}}}{(k_i)_{\text{geometrical}}} = \left(\frac{r'_0}{r_0}\right)^3 = \left(\frac{2\epsilon}{2\epsilon + I + 0}\right)^{1/2} \quad (\text{II.3})$$

Values given by Taylor-Glasstone⁽³⁷⁾ for the constants 2ϵ , I , and 0 are, respectively, 47, 10, and 190 for water and 93, 10, and 84 for ammonia. However, these values of 0 are for room temperature (293°K), and since we are generally interested in temperatures of 3000°K or higher, and since also in a mixture a water or ammonia molecule is not usually surrounded by polar molecules, rough effective values for 0 of 6 for water and 3 for ammonia were assumed. Using these values in (II.3), correction factors of 0.864 and 0.937 were obtained for water and ammonia, respectively. The covolumes corrected with these factors are given in parentheses in column three of the table.

Also given in Table II.1 are values based on r_0 values given by Taylor-Glasstone,⁽³⁷⁾ scaled so as to give the same covolume for N_2 as the geometrical value. These are room temperature values; hence the values for H_2O , NH_3 , and presumably also NO are quite small because of the large orientation effect.

The final values accepted for the covolumes (given in the last column of the table) are based primarily on the geometrical calculations, but with consideration given also to the Lennard-Jones r_0 values and to intuition. Thus the CO_2 value has been reduced somewhat as a concession to the much lower relative value which would be calculated for

5110



██████████

SECRET

this elongated molecule if rotation were not allowed, the values for OH and NO have been reduced 5 or 10% to allow for polar effects (estimated, for lack of data), the NH_3 value has been made slightly smaller than the corrected geometrical value since the Lennard-Jones r_0 value for NH_3 is even smaller than that for H_2O , and the CH_4 value has been reduced considerably since the Lennard-Jones r_0 value lies between the values for CO and N_2 . Although there is some arbitrariness in this procedure, the values are still felt to be good enough for the present purpose. (As has been emphasized before, the individual co-volume values have an appreciable effect on the calculated composition but very little influence on the shape of the calculated loading density curve.) It may be noted that the only important differences between our values and the Brinkley-Wilson values occur for the polar molecules, where Brinkley and Wilson have apparently been influenced by room-temperature values.

SECRET


-95-

██████████

Table II.1

Covolume Constants (k_i)

i	Species	Brinkley- Wilson(3,23)	Christian- Snay(7)	Pauling r	Lennard- Jones r_o	Final geometrical values
1	H ₂	153	60	170	188	180
2	CO ₂	687	525	737	721,568	670
3	CO	386	313	386	448	390
4	H ₂ O	108	285	417(360)	103	360
5	N ₂	353	334	376	376	380
6	NO	233		365	243	350
7	C(s)					
8	OH	108		250		230
9	O ₂	333		353	347	350
10	NH ₃	164		461(432)	100	420
11	CH ₄	400		529	410	450
12	C(g)			179		180
13	-C ₂ (g)			504		500



 3710

Appendix III

EQUATION-OF-STATE DATA FOR FOUR EXPLOSIVES

This appendix contains equation-of-state data for the following explosives:

63/35	RDX/TNT	($\rho_0 = 1.715$ g/cc),
77/23	RDX/TNT	($\rho_0 = 1.746$ g/cc),
76/24	HMX/TNT	($\rho_0 = 1.815$ g/cc),
	HMX	($\rho_0 = 1.900$ g/cc).

(The compositions are percentages by weight, not mole fractions.)

All data were calculated for equilibrium composition of the reaction products, using for the gaseous products the equation of state (2.2) with parameter values (6.10), and for the solid carbon the equation of state (2.4), (2.6). The data represent approximately $1\frac{1}{2}$ to 2 hours of 701 machine time per explosive.

Units for all results are:

$$p - Mb \quad (10^{12} \text{ dynes/cm}^2)$$

$$T - ^\circ K$$


$$e - Mb\text{-cc/g} \quad (10^{12} \text{ ergs/g})$$

$$s - 10^{-5} Mb\text{-cc/g-}^\circ K \quad (10^7 \text{ ergs/g-}^\circ K)$$

Internal energies are referred to an energy zero such that the energies of the elements are zero at $T = 0^\circ K$.

(Note: The tables which follow were made on IBM tabulators, which has made it necessary to represent p , e , and s by P , E , and S , respectively.)

3710



[REDACTED] 98
 [REDACTED]

TABLE III.1
 EQUATION OF STATE OF 65/35 RDX/TNT
 A. HUGONIOT

V/V ₀	P	T	E	S
0.400000	2.286944	13143.245	0.404099	9.234468
0.425000	1.826758	10374.083	0.310285	8.688241
0.450000	1.475962	8101.888	0.240720	8.191160
0.475000	1.214503	6499.388	0.189943	7.760607
0.500000	1.015264	5400.042	0.152048	7.394363
0.525000	0.858934	4638.086	0.122999	7.086108
0.550000	0.733696	4097.558	0.100308	6.831309
0.575000	0.632201	3702.718	0.082384	6.626273
0.600000	0.549370	3407.597	0.068117	6.466679
0.625000	0.481314	3183.826	0.056672	6.346953
0.650000	0.424986	3012.755	0.047416	6.261091
0.675000	0.378037	2882.108	0.039870	6.203368
0.700000	0.338560	2781.348	0.033662	6.168351
0.725000	0.305098	2703.481	0.028511	6.151416
C-J 0.742776	0.284330	2659.100	0.025373	6.148238
0.750000	0.276518	2643.242	0.024204	6.148718
0.775000	0.251930	2596.596	0.020576	6.157085
0.800000	0.230630	2560.470	0.017498	6.173966

98
 [REDACTED]

SECRET

TABLE III.1. CONT.

EQUATION OF STATE OF 65/35 RDX/TNT

B. C-J ADIABAT

V/V ₀	P	T	E	S
0.400000	1.799750	3635.169	0.174386	6.148238
0.425000	1.503704	3595.454	0.150380	6.148237
0.450000	1.265525	3531.582	0.130258	6.148237
0.475000	1.074120	3453.955	0.113253	6.148238
0.500000	0.919397	3370.162	0.098762	6.148235
0.525000	0.793286	3284.729	0.086309	6.148237
0.550000	0.689582	3200.269	0.075524	6.148237
0.575000	0.603560	3118.229	0.066118	6.148238
0.600000	0.531615	3039.376	0.057859	6.148237
0.625000	0.470983	2964.294	0.050563	6.148237
0.650000	0.419519	2893.039	0.044082	6.148238
0.675000	0.375532	2825.353	0.038296	6.148238
0.700000	0.337699	2761.170	0.033104	6.148238
0.725000	0.304969	2700.365	0.028425	6.148238
C-J 0.742776	0.284330	2659.100	0.025373	6.148238
0.750000	0.276500	2642.781	0.024192	6.148238
0.775000	0.251609	2588.247	0.020346	6.148238
0.800000	0.229744	2536.584	0.016841	6.148238
0.850000	0.193355	2441.171	0.010695	6.148240
0.900000	0.164570	2355.201	0.005493	6.148239
0.950000	0.141468	2277.477	0.001043	6.148239
1.000000	0.122691	2206.948	-0.002798	6.148238
1.050000	0.107252	2142.714	-0.006143	6.148238
1.100000	0.094429	2084.004	-0.009078	6.148238
1.150000	0.083680	2030.159	-0.011670	6.148238
1.200000	0.074595	1980.616	-0.013974	6.148238
1.250000	0.066857	1934.894	-0.016034	6.148237
1.300000	0.060220	1892.576	-0.017884	6.148238
1.350000	0.054493	1853.304	-0.019555	6.148238
1.400000	0.049520	1816.765	-0.021070	6.148238
1.450000	0.045180	1782.688	-0.022449	6.148238
1.500000	0.041371	1750.834	-0.023710	6.148237
1.550000	0.038013	1720.994	-0.024866	6.148238
1.600000	0.035040	1692.983	-0.025931	6.148237
1.700000	0.030036	1641.813	-0.027823	6.148237
1.800000	0.026019	1596.220	-0.029454	6.148238
1.900000	0.022751	1555.325	-0.030873	6.148238
2.000000	0.020059	1518.422	-0.032119	6.148238
4.000000	0.004176	1154.172	-0.042710	6.148238
6.000000	0.001849	1014.283	-0.045933	6.148238

SECRET

SECRET
TABLE III-1 - CONT.

EQUATION OF STATE OF 65/35 RDX/TNT

C. P AS A FUNCTION OF V AND E

V/V ₀ \ E	0.05	0.10	0.15
0.550000	0.643384	0.733145	0.824348
0.600000	0.517958	0.604492	0.692334
0.650000	0.429236	0.511454	0.595450
0.700000	0.363747	0.441703	0.521770
0.750000	0.313804	0.388014	0.463803
0.800000	0.274744	0.345629	0.416844
0.850000	0.243579	0.311331	0.377885
0.900000	0.218298	0.282955	0.342818
0.950000	0.197476	0.259031	0.310955
1.000000	0.180071	0.238542	0.283683
1.500000	0.090118	0.117138	0.140921
2.000000	0.055285	0.072719	0.088254
2.500000	0.038438	0.051059	0.062406
3.000000	0.028851	0.038647	0.047514
3.500000	0.022798	0.030759	0.038003
4.000000	0.018687	0.025371	0.031479

V/V ₀ \ E	0.20	0.25	0.30
0.400000	1.826970	1.929656	2.049467
0.425000	1.580132	1.688834	1.803477
0.450000	1.388598	1.496292	1.604971
0.475000	1.235097	1.339734	1.442423
0.500000	1.109643	1.210659	1.307471
0.525000	1.005702	1.102850	1.193914
0.550000	0.918587	1.011650	1.097121
0.575000	0.844751	0.933556	1.013627
0.600000	0.781471	0.865917	0.940826
0.650000	0.678672	0.754436	0.819848
0.700000	0.598542	0.666110	0.723196
0.750000	0.534068	0.594204	0.642612
0.800000	0.480885	0.531079	0.569928
0.850000	0.432214	0.475234	0.509741
0.900000	0.389728	0.428374	0.459301
0.950000	0.353676	0.388642	0.416580
1.000000	0.322799	0.354638	0.380050

SECRET

•••• : •••• ••

TABLE III.2
 EQUATION OF STATE OF 77/23 RDX/TNT
 A. HUGONIOT

V/V ₀	P	T	E	S
0.400000	2.462565	13551.856	0.427987	9.323819
0.425000	1.970174	10728.257	0.329278	8.769134
0.450000	1.591533	8333.095	0.255536	8.258195
0.475000	1.309339	6631.087	0.201715	7.812481
0.500000	1.095111	5470.706	0.161668	7.432397
0.525000	0.927347	4673.257	0.131008	7.111561
0.550000	0.792790	4110.818	0.107028	6.844842
0.575000	0.683442	3700.653	0.088044	6.628593
0.600000	0.593981	3394.059	0.072904	6.459035
0.625000	0.520355	3161.741	0.060745	6.331045
0.650000	0.459363	2984.632	0.050906	6.238779
0.675000	0.408507	2849.915	0.042884	6.176491
0.700000	0.365736	2746.601	0.036285	6.138505
0.725000	0.329487	2667.406	0.030812	6.119987
C-J 0.743261	0.306415	2621.526	0.027393	6.116368
0.750000	0.298535	2606.739	0.026238	6.116824
0.775000	0.271916	2560.346	0.022385	6.125620
0.800000	0.248866	2524.977	0.019118	6.143617

SECRET
 -101-
 [REDACTED]

UNCLASSIFIED

TABLE III.2 - CONT.

UNCLASSIFIED

EQUATION OF STATE OF 77/23 RDX/TNT

B. C-J ADIABAT

V/V ₀	P	T	E	S
0.400000	1.940786	3543.101	0.185687	6.116368
0.425000	1.624783	3520.514	0.160230	6.116367
0.450000	1.368429	3469.383	0.138863	6.116367
0.475000	1.161728	3400.251	0.120800	6.116368
0.500000	0.994415	3322.112	0.105404	6.116366
0.525000	0.857960	3240.503	0.092174	6.116366
0.550000	0.745718	3158.655	0.080718	6.116368
0.575000	0.652599	3078.405	0.070727	6.116368
0.600000	0.574710	3000.772	0.061956	6.116368
0.625000	0.509078	2926.726	0.054210	6.116368
0.650000	0.453358	2855.979	0.047330	6.116368
0.675000	0.405733	2788.617	0.041188	6.116368
0.700000	0.364773	2724.619	0.035679	6.116368
0.725000	0.329338	2663.894	0.030716	6.116368
C-J 0.743261	0.306415	2621.526	0.027393	6.116368
0.750000	0.298518	2606.306	0.026226	6.116368
0.775000	0.271574	2551.702	0.022148	6.116368
0.800000	0.247907	2499.918	0.018433	6.116368
0.850000	0.208526	2404.151	0.011920	6.116370
0.900000	0.177382	2317.728	0.006410	6.116369
0.950000	0.152396	2239.490	0.001701	6.116369
1.000000	0.132093	2168.414	-0.002362	6.116368
1.050000	0.115406	2103.614	-0.005899	6.116368
1.100000	0.101550	2044.329	-0.009000	6.116368
1.150000	0.089938	1989.907	-0.011738	6.116368
1.200000	0.080126	1939.787	-0.014169	6.116368
1.250000	0.071771	1893.489	-0.016342	6.116368
1.300000	0.064608	1850.600	-0.018292	6.116368
1.350000	0.058427	1810.760	-0.020052	6.116368
1.400000	0.053061	1773.660	-0.021647	6.116368
1.450000	0.048379	1739.027	-0.023099	6.116368
1.500000	0.044271	1706.623	-0.024424	6.116368
1.550000	0.040651	1676.240	-0.025640	6.116368
1.600000	0.037445	1647.692	-0.026757	6.116364
1.700000	0.032053	1595.469	-0.028742	6.116368
1.800000	0.027728	1548.851	-0.030450	6.116368
1.900000	0.024210	1506.961	-0.031935	6.116368
2.000000	0.021316	1469.092	-0.033236	6.116368
4.000000	0.004324	1090.379	-0.044179	6.116368
6.000000	0.001877	0941.993	-0.047427	6.116368

102

UNCLASSIFIED

TABLE 11:2 CONT.



UNCLASSIFIED

EQUATION OF STATE OF 77/23 RDX/TNT

C. P AS A FUNCTION OF V AND E

V/V ₀ \ E	0.05	0.10	0.15
0.550000	0.689734	0.780180	0.872128
0.600000	0.553508	0.641573	0.731078
0.650000	0.457843	0.541903	0.627758
0.700000	0.387463	0.467294	0.549458
0.750000	0.333901	0.409922	0.488123
0.800000	0.292063	0.364740	0.438636
0.850000	0.258699	0.328304	0.392776
0.900000	0.231643	0.298264	0.353679
0.950000	0.209377	0.271312	0.320566
1.000000	0.190794	0.246952	0.292250
1.500000	0.093754	0.120497	0.144466
2.000000	0.057286	0.074491	0.090194
2.500000	0.039697	0.052143	0.063635
3.000000	0.029716	0.039375	0.048364
3.500000	0.023429	0.031279	0.038628
4.000000	0.019168	0.025759	0.031959

V/V ₀ \ E	0.20	0.25	0.30
0.400000	1.949626	2.041869	2.163052
0.425000	1.677282	1.784166	1.901878
0.450000	1.470209	1.579070	1.691447
0.475000	1.305759	1.412624	1.519279
0.500000	1.171850	1.275557	1.376487
0.525000	1.061065	1.161227	1.256495
0.550000	0.968310	1.064676	1.154380
0.575000	0.889809	0.982152	1.066442
0.600000	0.822656	0.910815	0.989888
0.650000	0.713911	0.793553	0.862924
0.700000	0.629507	0.700915	0.756021
0.750000	0.561215	0.617579	0.663882
0.800000	0.497945	0.547859	0.588635
0.850000	0.445494	0.490067	0.526340
0.900000	0.401484	0.441593	0.474144
0.950000	0.364165	0.400506	0.429942
1.000000	0.332222	0.365354	0.392154

103



UNCLASSIFIED

SECRET

UNCLASSIFIED

TABLE III.3
EQUATION OF STATE OF 76/24 HMX/TNT
A. HUGONIOT

V/V ₀	P	T	E	S
0.400000	2.723679	13930.584	0.454802	9.357422
0.425000	2.182018	11047.336	0.350243	8.788203
0.450000	1.761759	8520.323	0.271541	8.256535
0.475000	1.448336	6710.429	0.214077	7.787889
0.500000	1.211430	5487.121	0.171471	7.386550
0.525000	1.026382	4657.320	0.138913	7.046486
0.550000	0.877615	4076.416	0.113402	6.761310
0.575000	0.756157	3652.149	0.093138	6.527237
0.600000	0.656420	3333.623	0.076940	6.341409
0.625000	0.574179	3091.769	0.063923	6.199569
0.650000	0.506039	2908.223	0.053398	6.096339
0.675000	0.449216	2768.869	0.044826	6.025777
0.700000	0.401468	2662.958	0.037786	5.982021
0.725000	0.361052	2582.699	0.031959	5.959861
C-J 0.746000	0.331752	2530.680	0.027820	5.954623
0.750000	0.326591	2522.108	0.027099	5.954801
0.775000	0.297000	2476.621	0.023016	5.963073
0.800000	0.271419	2442.763	0.019561	5.981600

SECRET

UNCLASSIFIED

TABLE III.3 - CONT.

UNCLASSIFIED

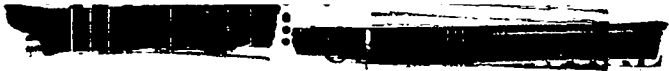
EQUATION OF STATE OF 76/24 HMX/TNT

B. C-J ADIABAT

V/V ₀	P	T	E	S
0.400000	2.161341	3325.152	0.197494	5.954623
0.425000	1.816153	3335.577	0.170157	5.954623
0.450000	1.529224	3311.310	0.147179	5.954623
0.475000	1.296139	3260.447	0.127774	5.954622
0.500000	1.107259	3195.080	0.111266	5.954622
0.525000	0.953355	3122.820	0.097108	5.954622
0.550000	0.826959	3048.089	0.084874	5.954623
0.575000	0.722293	2973.607	0.074226	5.954623
0.600000	0.634918	2900.913	0.064896	5.954623
0.625000	0.561401	2830.509	0.056671	5.954623
0.650000	0.499093	2762.849	0.049379	5.954623
0.675000	0.445926	2698.142	0.042880	5.954624
0.700000	0.400270	2636.452	0.037060	5.954623
0.725000	0.360835	2577.747	0.031824	5.954624
C-J 0.746000	0.331752	2530.680	0.027820	5.954623
0.750000	0.326584	2521.943	0.027095	5.954623
0.775000	0.296684	2468.924	0.022807	5.954623
0.800000	0.270456	2418.555	0.018904	5.954624
0.850000	0.226899	2325.197	0.012078	5.954625
0.900000	0.192536	2240.743	0.006318	5.954624
0.950000	0.165032	2164.132	0.001406	5.954624
1.000000	0.142731	2094.413	-0.002822	5.954624
1.050000	0.124439	2030.754	-0.006495	5.954624
1.100000	0.109280	1972.433	-0.009708	5.954624
1.150000	0.096598	1918.825	-0.012539	5.954623
1.200000	0.085900	1869.397	-0.015050	5.954624
1.250000	0.076805	1823.687	-0.017288	5.954623
1.300000	0.069019	1781.294	-0.019294	5.954623
1.350000	0.062311	1741.875	-0.021101	5.954624
1.400000	0.056496	1705.129	-0.022736	5.954624
1.450000	0.051429	1670.792	-0.024222	5.954623
1.500000	0.046989	1638.634	-0.025576	5.954623
1.550000	0.043082	1608.454	-0.026816	5.954623
1.600000	0.039627	1580.071	-0.027955	5.954623
1.700000	0.033826	1528.082	-0.029972	5.954621
1.800000	0.029183	1481.596	-0.031704	5.954623
1.900000	0.025417	1439.757	-0.033205	5.954623
2.000000	0.022325	1401.874	-0.034518	5.954623
4.000000	0.004384	1019.459	-0.045392	5.954623
6.000000	0.001867	868.690	-0.048532	5.954623

0110-105

UNCLASSIFIED



SECRET

EQUATION OF STATE OF 76/24 HMX/TNT

UNCLASSIFIED

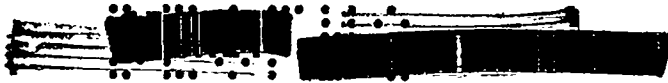
C. P AS A FUNCTION OF V AND E

V/V ₀ \ E	0.05	0.10	0.15
0.550000	0.763974	0.853796	0.945290
0.600000	0.607946	0.697411	0.788316
0.650000	0.500168	0.586216	0.673802
0.700000	0.421465	0.503442	0.587490
0.750000	0.361924	0.439972	0.520371
0.800000	0.315603	0.390187	0.466615
0.850000	0.278774	0.350262	0.421980
0.900000	0.248971	0.317544	0.379744
0.950000	0.224499	0.290200	0.343997
1.000000	0.204132	0.265071	0.313445
1.500000	0.100279	0.128823	0.154289
2.000000	0.061107	0.079405	0.096030
2.500000	0.042255	0.055455	0.067589
3.000000	0.031576	0.041798	0.051271
3.500000	0.024858	0.033152	0.040885
4.000000	0.020312	0.027266	0.033782

V/V ₀ \ E	0.20	0.25	0.30
0.400000	2.160695	2.230075	2.351003
0.425000	1.840303	1.940596	2.060880
0.450000	1.603595	1.711931	1.827915
0.475000	1.418611	1.527075	1.637703
0.500000	1.269149	1.375207	1.480299
0.525000	1.145946	1.248830	1.348419
0.550000	1.043018	1.142428	1.236580
0.575000	0.956104	1.051816	1.140635
0.600000	0.881980	0.973794	1.057425
0.650000	0.762609	0.846279	0.920129
0.700000	0.670698	0.746246	0.811281
0.750000	0.597538	0.664115	0.714109
0.800000	0.535053	0.588747	0.632695
0.850000	0.478397	0.526303	0.565331
0.900000	0.430885	0.473951	0.508920
0.950000	0.390616	0.429597	0.461175
1.000000	0.356163	0.391666	0.420379

SECRET

UNCLASSIFIED



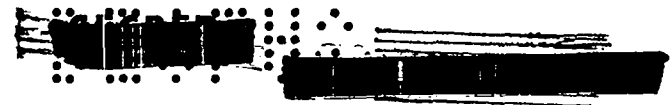


 UNCLASSIFIED

UNCLASSIFIED

TABLE III.4
 EQUATION OF STATE OF HMX
 A. HUGONIOT

V/V ₀	P	T	E	S
0.400000	3.227617	14809.120	0.515784	9.537179
0.425000	2.596288	11860.636	0.399018	8.947521
0.450000	2.096072	9054.157	0.309538	8.382373
0.475000	1.720646	6974.240	0.243880	7.871184
0.500000	1.439763	5585.797	0.195602	7.429602
0.525000	1.222705	4670.496	0.158997	7.054793
0.550000	1.048240	4044.172	0.130293	6.737355
0.575000	0.904577	3587.930	0.107329	6.471283
0.600000	0.785548	3243.249	0.088849	6.255050
0.625000	0.686819	2980.949	0.073937	6.086593
0.650000	0.604786	2783.357	0.061863	5.962019
0.675000	0.536245	2634.531	0.052022	5.875471
0.700000	0.478632	2523.210	0.043946	5.820886
0.725000	0.429886	2440.552	0.037269	5.792426
C-J 0.748055	0.391364	2383.871	0.032107	5.784796
0.750000	0.388362	2379.805	0.031709	5.784849
0.775000	0.352753	2335.831	0.027046	5.793635
0.800000	0.322015	2304.725	0.023107	5.815019



 UNCLASSIFIED

UNCLASSIFIED

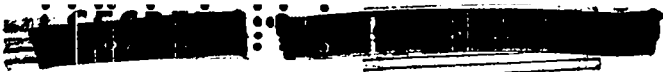


TABLE 11.4 - CONT.

UNCLASSIFIED

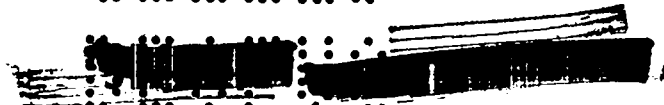
EQUATION OF STATE OF HMX

B. C-J ADIABAT

V/V ₀	P	T	E	S
0.400000	2.558204	2977.815	0.226796	5.784796
0.425000	2.175249	3008.371	0.195713	5.784796
0.450000	1.841779	3037.223	0.169326	5.784796
0.475000	1.561616	3024.445	0.146991	5.784795
0.500000	1.332700	2984.641	0.127998	5.784796
0.525000	1.145954	2930.335	0.111731	5.784796
0.550000	0.992698	2868.642	0.097693	5.784794
0.575000	0.865935	2803.780	0.085490	5.784796
0.600000	0.760231	2738.213	0.074811	5.784796
0.625000	0.671393	2673.390	0.065409	5.784796
0.650000	0.596178	2610.157	0.057083	5.784796
0.675000	0.532058	2548.992	0.049671	5.784796
0.700000	0.477045	2490.146	0.043040	5.784796
0.725000	0.429566	2433.729	0.037083	5.784796
C-J 0.748055	0.391364	2383.871	0.032107	5.784796
0.750000	0.388360	2379.760	0.031708	5.784796
0.775000	0.352415	2328.203	0.026839	5.784796
0.800000	0.320907	2278.988	0.022414	5.784796
0.850000	0.268636	2187.205	0.014684	5.784798
0.900000	0.227458	2103.586	0.008177	5.784797
0.950000	0.194547	2027.277	0.002639	5.784797
1.000000	0.167901	1957.469	-0.002118	5.784798
1.050000	0.146076	1893.431	-0.006240	5.784797
1.100000	0.128014	1834.511	-0.009840	5.784797
1.150000	0.112925	1780.141	-0.013005	5.784797
1.200000	0.100213	1729.822	-0.015805	5.784797
1.250000	0.089419	1683.120	-0.018297	5.784797
1.300000	0.080189	1639.660	-0.020526	5.784797
1.350000	0.072245	1599.112	-0.022529	5.784797
1.400000	0.065368	1561.189	-0.024338	5.784797
1.450000	0.059380	1525.640	-0.025978	5.784797
1.500000	0.054139	1492.243	-0.027470	5.784797
1.550000	0.049531	1460.804	-0.028833	5.784797
1.600000	0.045462	1431.151	-0.030082	5.784797
1.700000	0.038637	1376.603	-0.032288	5.784797
1.800000	0.033188	1327.564	-0.034173	5.784797
1.900000	0.028777	1283.205	-0.035800	5.784797
2.000000	0.025163	1242.854	-0.037216	5.784797
4.000000	0.004548	828.606	-0.048559	5.784797
6.000000	0.001821	668.563	-0.051586	5.784796

108

UNCLASSIFIED





SECRET

UNCLASSIFIED

EQUATION OF STATE OF HMX

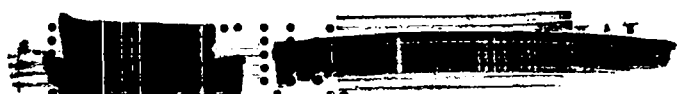
C. P AS A FUNCTION OF V AND E

V/V ₀ \ E	0.05	0.10	0.15
0.550000	0.914209	0.996592	1.083790
0.600000	0.714640	0.805559	0.898004
0.650000	0.583285	0.672762	0.763888
0.700000	0.489161	0.575216	0.663290
0.750000	0.418518	0.500793	0.582868
0.800000	0.363895	0.442558	0.514835
0.850000	0.320613	0.394700	0.458821
0.900000	0.285663	0.353634	0.412080
0.950000	0.256998	0.319050	0.372625
1.000000	0.233181	0.289623	0.338983
1.500000	0.110390	0.138616	0.165014
2.000000	0.066529	0.084657	0.101993
2.500000	0.045624	0.058735	0.071420
3.000000	0.033876	0.044045	0.053959
3.500000	0.026532	0.034791	0.042888
4.000000	0.021588	0.028515	0.035339

V/V ₀ \ E	0.20	0.25	0.30
0.400000	2.564922	2.579803	2.685376
0.425000	2.171131	2.224194	2.343100
0.450000	1.856913	1.951487	2.072350
0.475000	1.627630	1.734718	1.852730
0.500000	1.448724	1.558040	1.671579
0.525000	1.303632	1.411616	1.520211
0.550000	1.183280	1.288739	1.392257
0.575000	1.082008	1.184489	1.282894
0.600000	0.995892	1.095114	1.188429
0.650000	0.858007	0.948740	1.022915
0.700000	0.748261	0.822678	0.886656
0.750000	0.655763	0.721474	0.777289
0.800000	0.580450	0.638892	0.688105
0.850000	0.518214	0.570563	0.614373
0.900000	0.466131	0.513342	0.552673
0.950000	0.422064	0.464910	0.500485
1.000000	0.384416	0.423526	0.455918

SECRET

UNCLASSIFIED



UNCLASSIFIED

REPORT LIBRARY

MAR 1 1963

UNCLASSIFIED